View metadata, citation and similar papers at core.ac.uk

brought to you by CORE

provided by Texas A&M Repository

SUSY PHENOMENOLOGY

A Dissertation

by

BO HU

Submitted to the Office of Graduate Studies of
Texas A&M University
in partial fulfillment of the requirements for the degree of

DOCTOR OF PHILOSOPHY

August 2004

Major Subject: Physics

SUSY PHENOMENOLOGY

A Dissertation

by

BO HU

Submitted to Texas A&M University
in partial fulfillment of the requirements
for the degree of

DOCTOR OF PHILOSOPHY

Approved as to style and content by:

Richard Arnowitt (Chair of Committee)	
Christopher N. Pope (Member)	Ergin Sezgin (Member)
Stephen A. Fulling (Member)	Edward S. Fry (Head of Department)

August 2004

Major Subject: Physics

ABSTRACT

SUSY Phenomenology. (August 2004)

Bo Hu, B.S., Southwestern Jiaotong University;

M.S., Beijing Normal University

Chair of Advisory Committee: Dr. Richard Arnowitt

Supersymmetric extensions to the Standard Model (SM) have many interesting experimental consequences which can provide important hints to the physics beyond the SM. In this thesis, we first study the anomalous magnetic moment of the muon and show that a significant constraint on the parameter space can be obtained from its current experimental value. In the next topic, we study the CP violations in $B \to \phi K$ decays and show that the SM and the minimal supergravity model (mSUGRA) cannot account for the current experimental observation. We then show that all the data can be accommodated for a wide range of parameters in models with non-universal soft breaking left-right A terms. In our last topic, which is based on a Horava-Witten inspired model proposed by R. Arnowitt and B. Dutta, we extend their analysis to the full fermion sector of the SM and propose a new mechanism different from the usual see saw mechanism to generate small neutrino masses which are in good agreement with the current neutrino oscillation data.

To my parents

ACKNOWLEDGMENTS

I would like to thank Dr. Richard Arnowitt for his guidance and strong support during my graduate study at Texas A&M. I must also thank Dr. Bhaskar Dutta for his valuable contributions and generous sharing of knowledge. I also would like to thank Dr. Christopher N. Pope, Dr. Ergin Sezgin and Dr. Stephen A. Fulling for taking the time to be members of my graduate committee.

TABLE OF CONTENTS

CHAPTER Page

LIST OF TABLES

LIST OF FIGURES

FIGURE Page

CHAPTER I

INTRODUCTION

In the last three decades, particle physics achieved tremendous successes after the establishment of the Standard Model (SM) as the fundamental law governing low energy particle phenomena. The accuracy of its predictions has reached a few percent [1]. However, the SM has its intrinsic flaws and many unsolved problems, such as the hierarchy problem, the unification problem, the flavor problem, and so on [2]. Therefore, it has been long accepted that the SM, despite its remarkable achievement, is an effective theory describing physics at low energy. During the last two decades, many experiments were carried out or proposed to examine this idea. So far no evidence for physics beyond the SM has been found, but possible deviations from the SM predictions have been observed in recent experiments. Although we will have to wait for the Large Hadron Collider (LHC) to encounter new physics directly and to obtain first hand information, new physics can also manifest itself in many other places [3]. Not only can non-collider experiments provide useful hints of new physics and cross checks to the results obtained at colliders, some of them also are interesting and important at their own rights, e.g. solar neutrino experiments and experiments related to dark matter.

In this chapter we first introduce the SM and show that its problems lead to new physics including supersymmetric models (which will be discussed briefly in section 2). Then in section 3, we will discuss the phenomenological aspects of supersymmetric models. Details about the models considered in this thesis will be given in the next

---

The journal model is Nuclear Physics B.

chapter.

1. The Standard Model

The Standard Model of the strong, weak and electromagnetic interactions is a gauge theory based on the $SU(3)_C \times SU(2)_L \times U(1)_Y$ gauge group (see Appendix A for a short description). The electroweak symmetry breaking reduces this group to $SU(3)_C \times U(1)_{EM}$. The SM is extraordinarily successful not only because all the SM particles have been discovered except the Higgs boson, but also because a large amount of experimental data can be very well explained in its framework. However, theoretically the SM has many unsolved problems and unexplained elements:

- A large number of free parameters (19 in total, see Appendix A) which have to be measured experimentally.
- The unknown mechanism of the electroweak symmetry breaking (EWSB).
- The unexplained assignment of its gauge group.
- The unknown origin of its flavor structure and fermion mass spectrum.
- The hierarchy problem: radiative corrections to the Higgs mass, which is not protected by any symmetries, is quadratic and consequently requires either a ultraviolet cutoff at a low energy scale or unacceptable fine tunning if the validity of the SM is to be pushed to a scale beyond TeV.
- The problem that the unification of gauge couplings can not be achieved in the SM.
- The cosmological constant problem.

Experimentally no clear signal of new physics beyond the SM has been observed. Nevertheless, some possible deviations have been found:

- The baryon asymmetry and the dark matter content of the universe which cannot be explained in the SM. In the past this has not been considered as seriously as laboratory experiments due to the low accuracy in astrophysical measurements, but this situation has been changed significantly since the recent Wilkinson Microwave Anisotropy Probe (WMAP) experiment.

- Neutrino oscillations discovered at Super-Kamiokande [4] and Sudbury Neutrino Observatory (SNO) [5]. To explain their observations, neutrinos are required to possess very tiny masses which cannot be naturally explained by a slight modified version of the SM.

- The deviations of the anomalous magnetic moment of the muon [6, 7] and the CP asymmetry of the $B_0 \to \phi K_S$ [8, 9] decay from the SM predictions. Although the current experimental results of these two quantities are not extremely convincing, their sensitivity to physics beyond the SM makes them not only promising candidates to reveal the existence of new physics but also very useful for the purpose of constraining any given theory of new physics.

We will discuss neutrino oscillations, the anomalous magnetic moment of the muon and $B \to \phi K$ decays in detail in later chapters.

Naturally, the above discussions lead to the possibility that the SM needs certain extensions. However, it is very unlikely that one can discard the SM totally at low energy scale. Among all the theories proposed so far for new physics beyond the SM, supersymmetric theory discussed in the next section has long been considered as the most promising one due to its elegant solutions to many of the problems of the SM.

2. Supersymmetric models

Supersymmetry (SUSY) is defined through supersymmetric transformations which relate particles to their so-called superpartners with a change in spin by 1/2. In a theory which is invariant under supersymmetric transformations, i.e. supersymmetry being an exact symmetry of this theory, any particle and its superpartner must share the same mass. Since this is not observed, supersymmetry must be broken in nature. Although the mechanism of this breaking is unclear at this time, based on both theoretical and phenomenological considerations, SUSY models [10, 11, 12] with manifest broken supersymmetry still can be constructed. For example, the minimal supersymmetric standard model (MSSM) can be built by assigning a superpartner to each SM field and breaking SUSY via soft supersymmetry breaking terms which have to be constrained by experiments since both the theory breaking to the MSSM and the mechanism responsible for the breaking are unknown. Although SUSY has not been discovered and there exists many uncertainties (including some inherited from the SM) which presumably can be clarified by a more fundamental theory (e.g. string theory), the success of SUSY is remakable:

1. The hierarchy problem can be simply solved in the supersymmetric extensions to the SM because of the cancellation between the contributions of the SM fields and their superpartners to the Higgs mass.

2. The unification of gauge couplings can be achieved in supersymmetric grand unified theories (GUTs) where two distant scales, the electroweak ($\approx 10^{2-3}$ GeV) and the GUT scale ($\approx 10^{16}$ GeV), can be connected through renormalization group equations (RGEs). This provides us a way to investigate physics at very high energies which is far from accessible in current laboratories. For example, starting from a GUT theory which produces satisfactory low energy

results when compared with experimental measurements, it is possible to discuss physics at even higher scale, e.g. up to the Planck scale ($\approx 10^{18}$ GeV) (beyond which the quantum effects of gravity become important and a more fundamental theory has to take place). Therefore, SUSY leads us to not only the solutions to some of the problems of the SM, but also it leads to a much deeper understanding of nature and maybe (hopefully) the theory of everything.

3. The RGE running also provides a natural origin of the EWSB, which is usually referred as radiative electroweak symmetry breaking in literatures because it is the radiative corrections that cause the RGE running and drive related parameters to the values triggering the breaking.

4. The dark matter problem can be solved in R-parity conserved SUSY models where the lightest superpartner (LSP) is stable and can serve as the major constituent of the dark matter.

Besides these remarkable achievements of SUSY which are directly related to the problems of the SM, other advantages of SUSY can also be found. For example, invariance of a theory under local SUSY transformations will automatically bring gravitational interaction into the theory and thus provides a possible way to unify all known fundamental interactions. Moreover, SUSY is an indispensable component of string theory, which presumably can provide a full and consistence description of our microscopic world in the future. Many physicists believe that, no matter how our understanding evolves in the future, SUSY will be present in the final answer. It is partly because of this belief that SUSY phenomenology can grow into a very large and active research area even no clear signal of SUSY has been found so far.

3. SUSY phenomenology

Particle phenomenology is always closely related to experiments and SUSY phenomenology is not an exception. Since SUSY has not been found, looking for SUSY is one of the main tasks of the current particle experiments. Current experiments including those planned or proposed can be roughly divided into two categories:

1. Direct productions of SUSY particles at colliders and detection of SUSY particles existing in nature. Collider experiments have the advantage of being able to make accurate measurements. However detection experiments are more or less related to astrophysics to which collider experiments can not provide direct information.

2. Indirect searches (for a recent review, see [13]). Some important experiments in this category include the Brookhaven E821 experiment of the anomalous magnetic moment of the muon, the $b \to s\gamma$ and B decay experiments by BABAR, Belle and CLEO collaborations, WMAP measurement of the dark matter relic density, etc.

Although currently available experimental results can mostly be turned into certain constraints on SUSY models and we have to wait for Large Hadron Collider (LHC) to obtain accurate results, the examination of the current data cannot be overlooked since it provides the essential information about the models under study with implications for future experiments, including those at the LHC and those proposed for the Next Linear Collider (NLC). For example, the current $B_0 \to \phi K_S$ results from Belle and BABAR might be able to rule out the minimal supergravity (mSUGRA) model which has been discussed extensively and consequently require a non-minimal model which may have very different experimental signals. Some important results

will be presented in the next chapter after a more detailed introduction to the SUSY models studied in our work.

CHAPTER II

SUSY MODELS

We will focus on $N = 1$ and mostly dimension $D = 4$ models in the works presented in this thesis. N corresponds to the the number of spin 1/2 supersymmetry generators or charges that exist. These can be defined as:

$$Q|B\rangle \simeq |F\rangle; \quad Q|F\rangle \simeq |B\rangle \tag{2.1}$$

where B and F correspond to Bosonic states and Fermionic states, respectively. $N > 1$ supersymmetries cannot provide phenomenologically acceptable models and thus will not be considered here. In principal, one can construct theories with $D > 4$, which occurs in string models. However, for phenomenological studies $D = 4$ models are more relevant and in any event they can be considered as effective models compactified from higher dimensional fundamental theories. Although it is possible to construct models containing large extra dimensions (see, for example [14]) which can produce effects accessible in near future collider experiments and thus need to be explicitly considered, we will not discuss this type of model here since they are not relevant to our work.

In supersymmetric theories, fields are usually organized into supermultiplets, the irreducible representations of the supersymmetry algebra. Given supermultiplets and their gauge transformation properties, a low energy renormalizable supersymmetric theory can be determined by its superpotential, a dimension 3 holomorphic function of scalar fields. Details concerning the supersymmetric model building can be found in, e.g. [15, 16], and will not be discussed here. We will just briefly introduce models relevant to our works.

1. The MSSM

The MSSM is the minimal low energy supersymmetric extension to the SM. In our work it plays the role of the low energy effective theory at the electroweak scale.

As the minimal extension to the SM, its gauge group is the same as that of the SM, $SU(3)_C \times SU(2)_L \times U(1)_Y$. The MSSM superpotential can be written as:

$$W_Y = Y^{(u)} q_L H_2 u_R + Y^{(d)} q_L H_1 d_R + Y^{(e)} l_L H_1 e_R + \mu H_1 H_2. \tag{2.2}$$

where

$$q_L = \begin{pmatrix} u_L \\ d_r \end{pmatrix}; \quad l_L = \begin{pmatrix} \nu_L \\ e_r \end{pmatrix} \tag{2.3}$$

are the superpartners of the left handed quarks and leptons and u_R, d_R and e_R are the corresponding right handed ones. $H_{1,2}$ are the Higgs bosons. $Y^{u,d,e}$ are 3×3 superpotential Yukawa coupling matrices. μ is a parameter of mass dimension one. Both the Yukawa matrices and μ need not be real and hence can be possible sources of CP violations. In addition we assume here the conservation of R-parity which can be defined as

$$R = (-1)^{3(B-L)+2S} \tag{2.4}$$

where B, L and S correspond to the baryon number, lepton number and the spin, respectively. It is easy to check that under this definition the SM particles and Higgs are even and their superpartners are odd. R-parity conservation ensures that the superpartners must appear in pairs in any interaction and thus the lightest superpartner (LSP) must be stable.

As discussed in the last chapter, supersymmetry must be broken in any realistic theory. Since the mechanism responsible for the breaking is unknown, supersymmetry breaking is introduced phenomenologically by adding soft breaking terms manually

into the Lagrangian. By soft it means that those terms will not reintroduce the hierarchy problem which has already been solved in the case with unbroken supersymmetry. In fact even in the soft case it turns out that the soft mass parameters cannot be too large and should be roughly at the order of 1 TeV which is the region we are interested in. Given this requirement, the most general soft breaking Lagrangian can then be written as:

$$\begin{aligned} -\mathcal{L}_{soft}^{\text{MSSM}} &= \frac{1}{2}\sum_{\alpha=1}^{3} m_\alpha \lambda_\alpha \lambda_\alpha + m_{H_1}^2 |H_1|^2 + m_{H_2}^2 |H_2|^2 + m_{q_L}^2 q_L q_L^\dagger \\ &\quad + m_{l_L}^2 l_L l_L^\dagger + m_{u_R}^2 u_R u_R^\dagger + m_{d_R}^2 d_R d_R^\dagger + m_{e_R}^2 e_R e_R^\dagger \\ &\quad + [A^{(u)} Y^{(u)} q_L H_2 u_R + A^{(d)} Y^{(d)} q_L H_1 d_R \\ &\quad + A^{(e)} Y^{(e)} l_L H_1 e_R + \mu B H_1 H_2 + \text{h.c.}] \end{aligned} \tag{2.5}$$

where λ_α are gauginos, the superpartners of the gauge bosons. All the A's and m's are 3×3 complex matrices.

With its superpotential and soft breaking terms, the MSSM mass spectrum and interactions can be computed in a standard way which can be found in many papers (e.g. see [13, 16]). We will discuss this when necessary instead of presenting here the full story.

The advantage of the MSSM is that it represents the most general case of the minimal low energy supersymmetric model and is both of theoretical and phenomenological interest. However, as what can be seen from (2.2) and (2.3), it has a large number of parameters. Exact counting shows that it contains at least 105 new physical parameters [17] in addition to the SM parameters. Therefore, the advantage of the MSSM is more or less diluted by this large number of parameters. Nevertheless, it is still very useful in the sense that it can be used to make constraints on many parameters. Since many models at low energy, like those considered in this thesis,

have the same structure of the MSSM, they must satisfy the same constraints as the MSSM. So it is still the most frequently used model in SUSY phenomenological studies.

2. Minimal supergravity model

It is obvious from the discussion in the previous section that, if one works directly in the MSSM, all of its parameters have to be determined experimentally as was done with the SM parameters. In addition, assuming that the MSSM is the correct low energy model, the amount of the information needed for testing the validity of the MSSM to a high accuracy would be enormous and makes this test extremely complicated and impractical. One way out is to take the MSSM as the effective low energy theory of an underlying theory which has simpler structure at high energy. A large amount of work have been done in this direction and many models have been proposed. Here we concentrate on supergravity (SUGRA) models [10, 12, 15, 18], especially the minimal one, i.e. the minimal supergravity model (mSUGRA) [19, 20, 21, 22].

Supergravity incorporates gravity into the theory by requiring supersymmetry to be locally invariant. The full Lagrangian with unbroken supersymmetry can be constructed systematically. The result is too complicated (e.g. see [10]) to be displayed here. For phenomenological analysis it is good enough to take the limit of infinite Planck scale (i.e, the flat limit) which simplifies the Lagrangian to a form similar to that of the MSSM. The final structure strongly depends on the SUSY breaking mechanism since in the unbroken case symmetries can determine the structure. One phenomenologically acceptable SUSY breaking mechanism is to first break SUSY in a hidden sector and then communicate the breaking to the observable sector by gravity

[19]. mSUGRA discussed below is the minimal picture of this model.

In mSUGRA, at the GUT scale, the parameters of the soft breaking terms include a universal scalar mass m_0, a universal gaugino mass $m_{1/2}$ and the parameter A_0 of the cubic scalar terms, corresponding to setting the following in (2.5):

$$\begin{aligned} & m_\alpha = m_{1/2} \ ; \\ & m_{H_1}^2 = m_{H_2}^2 = m_{q_L}^2 = m_{l_L}^2 = m_{u_R}^2 = m_{d_R}^2 = m_{e_R}^2 = m_0^2 \ ; \\ & A^{(u)} = A^{(d)} = A^{(e)} = A_0 \ . \end{aligned} \tag{2.6}$$

Then we are left with 5 parameters (notice that in (2.5) there are two more parameters, μ and B). One can further require that the electroweak symmetry breaks radiatively to eliminate one more parameter. At the tree level, this requirement will give, at the electroweak scale,

$$\frac{1}{2}M_Z^2 = \frac{m_{H_1}^2 - m_{H_2}^2 \tan^2\beta}{\tan^2\beta - 1} - \mu^2 \tag{2.7}$$

and

$$B\mu = \frac{1}{2}(m_{H_1}^2 + m_{H_2}^2 + 2\mu^2)\sin 2\beta \tag{2.8}$$

where $\tan\beta = \langle H_2\rangle/\langle H_1\rangle$, the ratio between the vacuum expectation values (VEVs) of H_2 and H_1. (2.7) shows that μ^2 can be traded for $\tan\beta$ and then B can be eliminated. Notice that the sign of μ cannot be determined by (2.7) and needs to be specified at the weak scale. (In conventional mSUGRA, the soft breaking terms are assumed real). Therefore, we have four new parameters and a sign in addition to the SM parameters. In addition, when R-parity conservation is assumed, the superpotential in the mSUGRA model is the same as the MSSM one given in (2.2).

The studies of the mSUGRA model usually start with a set of parameters at the GUT scale and then run the renormalization group equations (REGs) [23, 24, 25, 26]

down to the electroweak scale. The SM parameters in many cases can be taken from the results of their SM fits at least as good approximations. In some cases, SUSY corrections are significant and thus have to be taken into account, e.g. SUSY corrections to the Higgs mass [27] and the mass of the bottom quark, m_b [28, 29].

Compared with the MSSM with more than 100 new parameters, mSUGRA has a much higher predictive power. Further, in mSUGRA, many analyses can be done in a more complete and accurate way. For example, the mass insertion approximation [30], which is not necessary in the mSUGRA case, is often used in the MSSM in flavor changing processes. As a consequence, the mSUGRA parameter space can be studied in an explicit way and correlations between experiments can be seen more clearly. In addition, many of its variations can be studied without losing much of its predictive power, e.g. models with non-universal soft scalar masses, gaugino masses, off-diagonal terms, etc.

3. Experimental constraints

In this section we give a general overview of some important experimental constraints on the mSUGRA parameter space. Their specific effects related to our work will be discussed later. The constraints on the MSSM can be found in [13] and will be skipped here since we will not work in the MSSM directly.

3.1. Limits on superpartner masses

The non-observation of any non-SM particles in collider experiments can establish the lower limits on superpartner masses. For example (for a complete list, see [1]), the current lower limit on the lightest neutralino mass, $m_{\tilde{\chi}^0}$, is 37 GeV at 95% confidence level, and the lighest chargino masses, $m_{\tilde{\chi}_1^\pm}$, ~ 100 GeV. However, since in most cases

the part of the parameter space below those limits has already been excluded by some other experimental constraints, e.g. those on the $b \to s\gamma$ branching ratio and the mass of the Higgs boson, they usually do not play an important role in constraining the mSUGRA parameter space. Nevertheless, the important issue is that no non-SM particle has been observed and no new physics theory can skip that test.

3.2. The lightest Higgs mass, m_h

The Higgs boson is the only SM particle not yet found. The Higgs boson by itself is an important issue since it is required by the Higgs mechanism of the gauge symmetry breaking in the SM. It is the Higgs mass that manifests the hierarchy problem. In addition, SUSY models require a very light Higgs (see [31] for a recent review) close to the current bound [32]:

$$m_h > 114.4 \ \text{GeV}, \tag{2.9}$$

which is a significant constraint on the parameter space at low $\tan\beta$. Due to the uncertainties in theoretical calculations and the top mass, the above bound is usually relieved by a few GeV, e.g. in the theoretical calculations we impose

$$m_h > 111 \ \text{GeV}. \tag{2.10}$$

3.3. $b \to s\gamma$

The current world average of the inclusive $B \to X_s\gamma$ branching ratio [33] is

$$\text{Br}(B \to X_s\gamma) = (3.34 \pm 0.38) \times 10^{-4} \tag{2.11}$$

which agrees with the latest SM theoretical prediction with full Next-to-Leading-Order QCD corrections [34]:

$$\text{Br}(B \to X_s\gamma) = (3.73 \pm 0.30) \times 10^{-4}. \tag{2.12}$$

By comparing (2.11) with (2.12), one can see that new physics contributions to $\mathrm{Br}(B \to X_s\gamma)$ are strongly constrained. In our works we use a relatively broad range to take into account the uncertainty in the theoretical calculation:

$$2.2 \times 10^{-4} < \mathrm{Br}(B \to X_s\gamma) < 4.5 \times 10^{-4}. \tag{2.13}$$

At large $\tan\beta$ it sets a lower bound on $m_{1/2}$ for $m_0 \lesssim 1$ TeV [1]. In addition, it strongly constrains the flavor changing $b \to s$ transition, especially in non-universal models.

The direct CP asymmetry of $b \to s\gamma$ also has been measured by CLEO [35]:

$$\mathcal{A}_{b\to s+\gamma} = (-0.079 \pm 0.108 \pm 0.022)(1.0 \pm 0.030) \tag{2.14}$$

or at 90% confidence level, $-0.27 < \mathcal{A}_{b\to s+\gamma} < +0.10$. We will consider this in our later discussion on $B \to \phi K$ decays.

3.4. The dark matter relic density

One intriguing and open question in modern cosmology is the nature of the dark matter which has been found to be the dominant matter component of the current universe. (For a review see [36]). The recent WMAP result gives [37]

$$\Omega_{CDM}h^2 = 0.1126^{+0.008}_{-0.009}\ . \tag{2.15}$$

where Ω_{CDM} is the ratio of the current dark matter mass density to the critical mass density and h is defined by the Hubble constant as $H_0 = 100\,h\,\mathrm{km\,s^{-1}Mpc^{-1}}$. We implement this bound at the 2σ level in our calculation:

$$0.094 < \Omega_{CDM}h^2 < 0.129\ . \tag{2.16}$$

[1] There is also the LEP bound $m_{\tilde{\chi}_i^\pm} > 103$ GeV which produces a lower bound on $m_{1/2}$ for any m_0 (not just $m_0 \lesssim 1$ TeV)

As explained in the first section, the LSP in an R-parity conserved model is stable and hence can be considered as a cold dark matter (CDM) candidate. By assuming that the stable LSP is the main ingredient of the dark matter, the above bound can then be translated into the constraint on the nature of the LSP and consequently the model producing this LSP. In mSUGRA, it turns out that the dark matter relic density can significantly reduce the parameter space to very narrow bands. One example is given in Fig. 1 below.

3.5. The muon anomalous magnetic moment

The current world average of the muon anomalous magnetic moment, $a_\mu = (g_\mu - 2)/2$, is [7]

$$a_\mu^{\rm EXP} = 11659208(6) \times 10^{-10} \tag{2.17}$$

which has a remarkable accuracy, 0.5 ppm (part per million). However, in theoretical calculations, the hadronic contribution is still not well determined due to the discrepancy in the experimental data used in the evaluation of the hadronic vacuum polarization contribution to the photon propagator [38, 39]. The most recent SM prediction using direct experimental $e^+e^- \to$ hadrons data gives [40]

$$a_\mu^{\rm SM}(e^+e^-) = (11659180.9 \pm 8.0) \times 10^{-10} \ . \tag{2.18}$$

On the other hand, the one using τ decay data gives [40]

$$a_\mu^{\rm SM}(\tau) = (11659195.6 \pm 6.8) \times 10^{-10} \ . \tag{2.19}$$

Therefore, comparing (2.17) to (2.18) and (2.19), one finds that [40]

$$\Delta a_\mu = a_\mu^{\rm EXP} - a_\mu^{\rm SM} = \begin{cases} 27.1 \pm 10.0 \times 10^{-10} & (e^+e^- \ \text{data}) \\ 12.4 \pm 9.0 \ \times 10^{-10} & (\tau \ \text{data}) \end{cases} \tag{2.20}$$

corresponding to 2.7σ and 1.4σ for e^+e^- and τ data, respectively.

Δa_μ given in (2.20) can be used as a bound on non-SM contributions to a_μ. In mSUGRA its lower (higher) bound produces a higher (lower) bound on m_0 and $m_{1/2}$. Even if there is no deviation from the SM, the bound is still significant, although a large deviation would be more welcome, for it would signal the existence of new physics. More details will be given in the next chapter devoted to the muon $g-2$.

3.6. Neutron and electron electric dipole moments

Usually in mSUGRA, for simplification, vanishing CP violating phases are assumed because their effects in most applications are small. However, in general they can be present and are hard to prevent from being large. Therefore, they must be considered in any CP violating processes.

Currently the most significant constraints on CP violating phases are from experimental measurements of the neutron and electron electric dipole moments (EDMs). In SUSY models, an electron EDM arises from the diagrams involving intermediate chargino-sneutrino states and intermediate neutralino-selectron states (for example, see [41, 42]). The current experimental bounds on the neutron and electron EDMs are [1]:

$$d_n < 6.3 \times 10^{-26}\ \mathrm{e\,cm}, \quad d_e < 0.21 \times 10^{-26}\ \mathrm{e\,cm}\ . \tag{2.21}$$

Besides those experimental constraints mentioned above, there are other phenomenological constraints which are very important in models like the MSSM but not the mSUGRA model. For example, flavor changing neutral currents (FCNCs). However, if one tries to extend mSUGRA, e.g. to include non-universal terms, these constraints in general need to be included.

Fig. 1 below shows how the mSUGRA parameter space gets constrained by the experimental data [43] for the case $A_0 = 0$, $\mu > 0$ and $\tan\beta = 40$. In Fig. 1, the

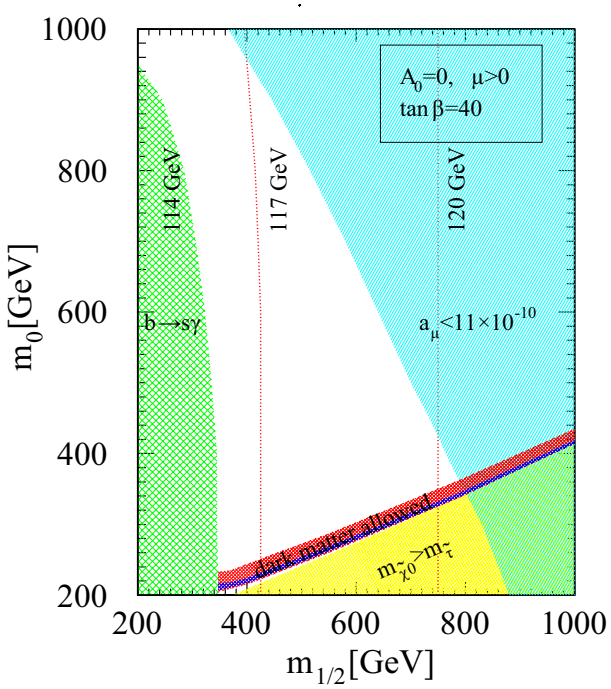

Fig. 1. Allowed region in the m_0 - $m_{1/2}$ plane from the relic density constraint for $\tan\beta = 40$, $A_0 = 0$ and $\mu > 0$.

red region was allowed by the older balloon data on the dark matter relic density, and the narrow blue band by the recent WMAP data. The dotted red vertical lines are different Higgs masses. The light green region to the left is excluded by the $B \to X_s\gamma$ bound. The light blue region is excluded if $\Delta a_\mu > 11 \times 10^{-10}$. The yellow region is excluded because in that region, instead of the neutralino, the LSP is the lightest slepton, the stau, which is charged and hence cannot be the cold dark matter component. Notice that the dark matter allowed region (the narrow blue band) is so narrow that it can approximately determine m_0 for a given $m_{1/2}$ for fixed A_0 and $\tan\beta$, and vice-versa.

CHAPTER III

MUON ANOMALOUS MAGNETIC MOMENT*

Any particle with spin possesses an magnetic moment which can be expressed in terms of the Landé g factor. Fig. 2 shows diagrammatically the contributions to g for the muon.

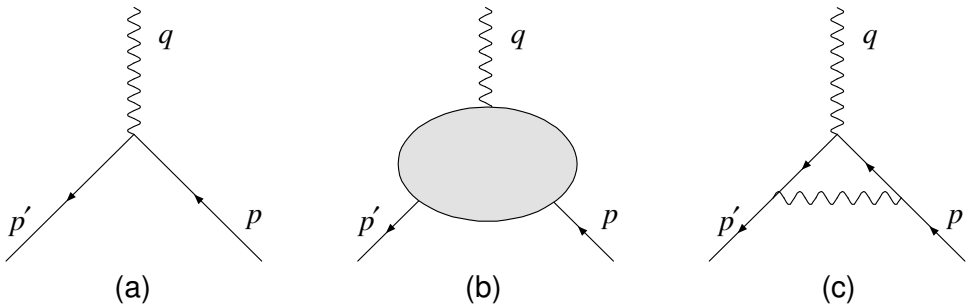

Fig. 2. (a) The lowest order contribution to the muon magnetic moment. (b) Diagrammatic representation of higher order contributions. (c) First order QED contribution, as an example of (b).

To the lowest order, as shown in Fig. 2(a), $g = 2$. Higher order loop contributions can be represented schematically by Fig. 2.(b). In general, g can be defined by the muon-photon vertex [44]

$$\bar{u}(p') \left[\frac{(p+p')_\mu}{2m} + \frac{g}{2} \frac{i\sigma_{\mu\nu} q^\nu}{2m} \right] u(p) \; . \tag{3.1}$$

When $g = 2$ one recovers the tree level vertex $\bar{u}(p')\gamma_\mu u(p)$. The anomalous contribution to the magnetic moment of the muon is usually defined as

$$a_\mu \equiv (g_\mu - 2)/2 \; . \tag{3.2}$$

*Tables and figures presented in this chapter are reprinted with permission from "Muon $g-2$, Dark Matter Detection and Accelerator Physics" by R. Arnowitt, B. Dutta, B. Hu, 2001, Phys. Lett. B 505, 177-183. Copyright 2001 by Elsevier.

The QED calculation shown in Fig. 2(c) was first done by Schwinger [45] in 1948. Later, with the improvement of experimental techniques, higher order QED contributions and non-QED contributions were calculated. We summarize below the current status of the SM prediction for a_μ.

1. muon $g-2$ in the SM

The SM contribution to a_μ can be written as the sum of the QED, electroweak and hadronic contributions

$$a_\mu^{\rm SM} = a_\mu^{\rm QED} + a_\mu^{\rm EW} + a_\mu^{\rm had} \ . \tag{3.3}$$

The dominant contribution to $a_\mu^{\rm SM}$ is $a_\mu^{\rm QED}$ which can be expresses in a power serial of α ($\equiv e^2/4\pi$)

$$a_\mu^{\rm QED} = \sum_{i=1}^{5} C_i \left(\frac{\alpha}{\pi}\right)^i + O(\alpha^6) \tag{3.4}$$

where $C_1 = 1/2$ which is Schwinger's original result. C_{2-5} also have been calculated. The current theoretical value of $a_\mu^{\rm QED}$ is [40]

$$a_\mu^{\rm QED} = 11658470.6(0.3) \times 10^{-11} \ . \tag{3.5}$$

The electroweak contribution is small but not negligible compared to the experimental accuracy [40]

$$a_\mu^{\rm EW} = 15.4(0.2) \times 10^{-10} \ . \tag{3.6}$$

$a_\mu^{\rm had}$ can be further divided into three parts:

$$a_\mu^{\rm had} = a_\mu^{\rm had,\ LO} + a_\mu^{\rm had,\ NLO} + a_\mu^{\rm had,\ l\text{-}b\text{-}l} \tag{3.7}$$

where the first two terms are the leading order and next-to-leading order hadronic vacuum polarization contributions and the last term is the hadronic light-by-light contribution [46]. The last two terms in (3.7) have been calculated to be [40]

$$a_\mu^{\text{had, NLO}} = -10.0(0.6) \times 10^{-10} \; ; \; a_\mu^{\text{had, l-b-l}} = 8.6(3.5) \times 10^{-10} \; . \tag{3.8}$$

However, the ambiguity in the evaluation of the leading order hadronic contribution, $a_\mu^{\text{had, LO}}$, has not yet been clarified. There are two different results based on different experimental data used in the analyses

$$a_\mu^{\text{had, LO}} = \begin{cases} 696.3(7.2) \times 10^{-10} & (e^+e^- \text{ data [40]}) \\ 711.0(5.8) \times 10^{-10} & (\tau \text{ data [40]}) \end{cases} \tag{3.9}$$

Collecting all the SM contributions given above, one finds the results given in (2.18)-(2.20).

2. muon $g-2$ in mSUGRA

Before the advent of supergravity grand unified models in 1982 [19, 20, 21, 22], efforts had been made to calculate a possible deviation from a_μ^{SM} within the framework of global supersymmetry [47, 48, 49, 50, 51]. However, it had been shown many years ago [51] that the anomalous magnetic moment vanishes in the limit of exact global supersymmetry, and thus one needs broken supersymmetry to obtain a non-zero result. The absence of a phenomenologically viable way of spontaneously breaking global supersymmetry made realistic predictions for these models difficult. On the contrary, spontaneous breaking of supersymmetry in supergravity (SUGRA) is easy to achieve. The first complete analysis [52] in supergravity unified models was done in 1984 by Yuan et al.

In SUGRA models, the spontaneous breaking of supersymmetry triggers the radiative electroweak symmetry breaking and hence the scale of the new SUSY masses

is required to be $\sim$ 100 GeV - 1 TeV, leading to the prediction [52] that the SUGRA contributions to the anomalous muon magnetic moment, $a_\mu^{\rm SUGRA}$, would be comparable or larger than the electroweak contribution given in (3.6), $15.4(2) \times 10^{-10}$. This scale for the SUSY masses was further confirmed by the LEP data showing that consistency with grand unification could be obtained if the SUSY masses also lie in the above range [53]. In addition, SUGRA models with R-parity invariance predict a dark matter candidate (the lightest neutralino) with the astronomically observed amount of relic density if the SUSY masses again lie in this range.

It is thus reasonable to investigate whether the observed deviation from $a_\mu^{\rm EXP}$ can be understood within the framework of SUGRA models, and here[1] we consider gravity mediated SUSY breaking with R-parity invariance for models with universal soft breaking masses (mSUGRA).

SUGRA models have a wide range of applicability including cosmological phenomena and accelerator physics, and constraints in one area affect predictions in other areas. In particular, as first observed in [55] and emphasized in [56], that a_μ increases with $\tan\beta$, as do dark matter detection rates. Thus as we will see, the deviation of (2.20) will significantly affect the minimum neutralino-proton cross section for terrestrial detectors. Even more significant is the fact that the astronomical bounds on the $\tilde{\chi}_1^0$ relic density restrict the SUSY parameter space and hence the SUGRA predictions

[1]This work was done in 2001 [54]. Since that time both the experimental measurement and the theoretical evaluations of a_μ have been improved. The ambiguity in $a_\mu^{\rm had,\,LO}$ (see section 1) found later after this work has led to an uncertain bound on $a_\mu^{\rm NP}$ (NP means new physics). Therefore, currently the bound on $a_\mu^{\rm SUSY}$ is usually used as an "optional" bound. However, once the $a_\mu^{\rm had,\,LO}$ problem is resolved, our discussion here is still valid (after making certain changes in our numerical results). Considering the ambiguity in $a_\mu^{\rm SM}$ and that the bound based on the more reliable e^+e^- data (see (2.20)) does not deviate very much from the one used in this work, we do not update our numerical results here. All other discussion should apply in future analyses.

for a_μ as well as what may be expected to be seen at the Tevatron RUN II and the LHC. In order to carry out this analysis, when applying the experimental bounds, we include all the co-annihilation effects, as well as the large $\tan\beta$ corrections to m_b and m_τ (which are needed to correctly determine the corresponding Yukawa coupling constants), the large $\tan\beta$ NLO corrections to the $b \to s\gamma$ decay [57, 58] and the one and two loop corrections to the light Higgs (h) mass. The above corrections for dark matter (DM) calculations were carried out in [59], and we will use the same corrections here.

Before proceeding on, we state the range of parameters we assume [2]. For $a_\mu^{\rm SUSY}$ We take a 2σ bound

$$11 \times 10^{-10} < a_\mu^{\rm SUSY} < 75 \times 10^{-10}\,, \tag{3.10}$$

a 2σ bound on the $b \to s\gamma$ branching ratio, $1.8\times10^{-4} < BR(b \to s\gamma) < 4.5\times10^{-4}$, and a neutralino relic density range of $0.02 < \Omega_{\tilde\chi_1^0} h^2 < 0.25$. (Assuming a lower bound of 0.1 does not affect results significantly.) The b-quark mass is assumed to have the range $4.0\,{\rm GeV} < m_b(m_b) < 4.4$ GeV. We also consider the bound on the Higgs mass: $m_h > 114$ GeV, which is the current LEP bound. However, the theoretical calculations of m_h have still some uncertainty as well as uncertainty in the t-quark mass, and so we will conservatively interpret this bound to mean that our theoretical values obey $m_h > 111$ GeV. (Our calculations of m_h are consistent with [60].) The scalar and gaugino masses at the GUT scale obey $(m_0, m_{1/2}) < 1$ TeV. We examine the range $2 < \tan\beta < 40$, and the cubic soft breaking mass is parameterized at the GUT scale by $|A_0| < 4m_{1/2}$.

[2] Similar to what happened to a_μ, as explained in footnote 1 on the last page, some experimental bounds used here are different from those given in chapter II (which was only intended to be a survey of some important experimental constraints), mostly due to the improvement in experimental measurements over the time passed after this work was complete.

We consider first the mSUGRA model, which depends on the four parameters m_0, $m_{1/2}$, A_0, $\tan\beta$ and the sign of the μ parameter, as described in chapter I. The SUSY contribution to a_μ arises from two types of loop diagrams, i.e. those with chargino-sneutrino intermediate states, and those with neutralino-selectron intermediate states, both of which are shown in Fig. 3 below.

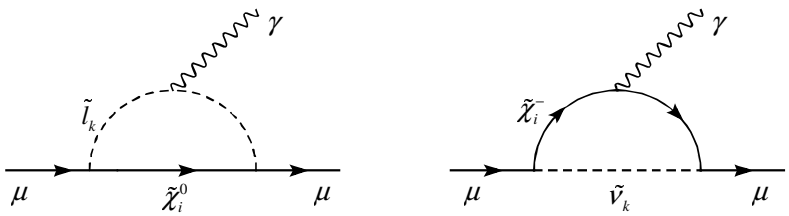

Fig. 3. SUSY contributions to a_μ: neutralino-selectron loop (left) and chargino-sneutrino loop (right).

The dominant contribution arises from the loop diagram with the light chargino ($\tilde{\chi}_1^\pm$). For moderate or large $\tan\beta$, and when $(\mu \pm \tilde{m}_2)^2 \ll M_W^2$, one finds

$$a_\mu^{\rm SUGRA} \cong \frac{\alpha}{4\pi}\frac{1}{\sin^2\theta_W}\left(\frac{m_\mu^2}{m_{\tilde{\chi}_1^\pm}\mu}\right)\frac{\tan\beta}{1-\frac{\tilde{m}_2^2}{\mu^2}}\left[1-\frac{M_W^2}{\mu^2}\frac{1+3\frac{\tilde{m}_2^2}{\mu^2}}{\left(1-\frac{\tilde{m}_2^2}{\mu^2}\right)^2}\right]F(x) \qquad (3.11)$$

where $\tilde{m}_i = (\alpha_i/\alpha_G)m_{1/2}$, $i = 1, 2, 3$ are the gaugino masses at the electroweak scale and $\alpha_G \cong 1/24$ is the GUT scale gauge coupling constant. (One has $m_{\tilde{\chi}_1^\pm} \cong \tilde{m}_2 \cong 0.8m_{1/2}$, and the gluino ($\tilde{g}$) mass is $m_{\tilde{g}} \cong \tilde{m}_3$.) The form factor in (3.11) is

$$F(x) = (1-3x)(1-x)^{-2} - 2x^2(1-x)^{-3}\ln x \qquad (3.12)$$

where $x = (m_{\tilde{\nu}}/m_{\tilde{\chi}^\pm})^2$. The sneutrino and chargino masses are related to m_0 and $m_{1/2}$ by the renormalization group equations. (The contribution from the heavy chargino, $\tilde{\chi}_2^\pm$ reduces this result by about a third.) One finds for large $m_{1/2}$ that $F(x) \cong 0.6$ so that a_μ decreases as $1/m_{1/2}$, while for large m_0, F decreases as $\ln(m_0^2)/m_0^2$ (exhibiting the SUSY decoupling phenomena).

One important consequence of (3.11) is that the sign of $a_\mu^{\rm SUGRA}$ is given by the sign of μ. The a_μ bound in (3.10) thus implies that μ is positive. This then has immediate consequences for dark matter detection. As discussed in [59, 61], for $\mu < 0$, accidental cancellations can occur reducing the neutralino-proton cross section to below 10^{-10} pb over a wide range of SUSY parameters, and making halo neutralino dark matter unobservable for present or future planned terrestial detectors. Thus this possibility has now been eliminated, and future detectors (e.g. GENIUS) should be able to scan almost the full SUSY parameter space for $m_{1/2} < 1$ TeV.

The lower bound in (3.10) plays a central role in limiting the $\mu > 0$ SUSY parameter space, particularly when combined with the bounds on the Higgs mass and the $b \to s\gamma$ constraints. As seen above, lowering $\tan\beta$ can be compensated in a_μ by also lowering $m_{1/2}$. However, m_h decreases with both decreasing $\tan\beta$ and decreasing $m_{1/2}$. Thus the combined Higgs and a_μ bounds put a lower bound on $\tan\beta$. This bound is sensitive to A_0 since A_0 enters in the L-R mixing in the stop (mass)^2 matrix and affects the values of the stop masses. We find for $m_h > 111$ GeV (i.e. the 114 GeV experimental bound), that $\tan\beta > 7$ for $A_0 = 0$, and $\tan\beta > 5$ for $A_0 = -4m_{1/2}$. At higher m_h the bound on $\tan\beta$ is more restrictive. Thus for $m_h > 117$ GeV (corresponding to an experimental 120 GeV bound), one has $\tan\beta > 15$ for $A_0 = 0$, and $\tan\beta > 10$ for $A_0 = -4m_{1/2}$. As the Higgs mass increases, the bound on $\tan\beta$ increases. For large $\tan\beta$, the relic density constraints leave only co-annihilation regions possible [59, 62, 63], and these are very sensitive to the value of A_0.

Fig. 4 exhibits the allowed regions in the $m_0 - m_{1/2}$ plane for $\tan\beta = 40$, $m_h > 111$ GeV for $A_0 = 0$, $-2m_{1/2}$, and $4m_{1/2}$ (from bottom to top). The corridors terminate at low $m_{1/2}$ due to the $b \to s\gamma$ and m_h constraints. Without the a_μ constraint, the corridors would extend up to the end of the parameter space ($m_{1/2} = 1$ TeV). We

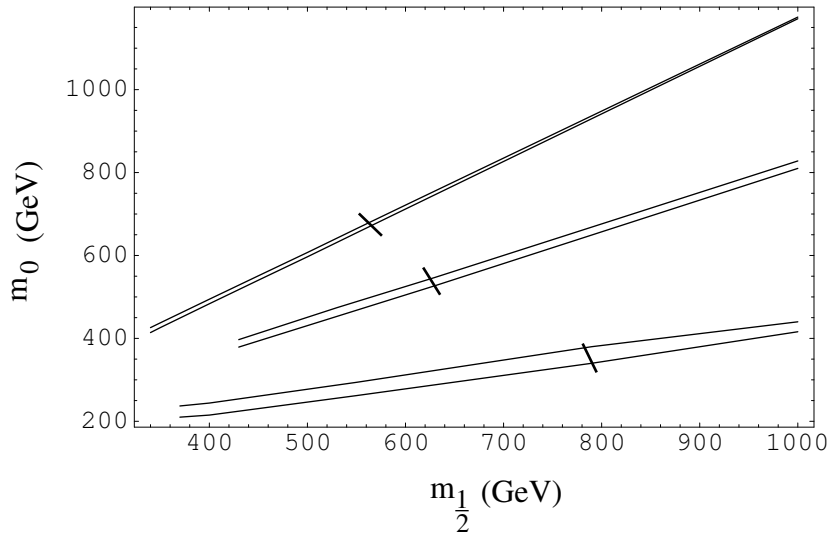

Fig. 4. Corridors in the $m_0 - m_{1/2}$ plane allowed by the relic density constraint for $\tan\beta = 40$, $m_h > 111$ GeV, $\mu > 0$ for $A_0 = 0, -2m_{1/2}, 4m_{1/2}$ from bottom to top. The curves terminate at low $m_{1/2}$ due to the $b \to s\gamma$ constraint except for the $A_0 = 4m_{1/2}$ which terminates due to the m_h constraint. The short lines through the allowed corridors represent the high $m_{1/2}$ termination due to the lower bound on a_μ.

see also that the relic density constraint effectively determines m_0 in terms of $m_{1/2}$ in this region. The lower bound of (3.10), however, cuts off these curves (at the vertical lines) preventing m_0 and $m_{1/2}$ from getting too large. Thus for large $\tan\beta$, the $g_\mu - 2$ experiment puts a strong constraint on the SUSY parameter space. As explained above, the restriction of the SUSY parameter space by the a_μ constraint affects the predicted dark matter detection rates. The exclusion of the large m_0 and large $m_{1/2}$ domain of Fig. 4 generally raises the lower bounds on the neutralino-proton cross section and hence the remain parameter space should generally be accessible to future planned detectors.

In non-universal cases, both the neutralino-proton cross section and neutralino dark matter relic density are affected by the non-universalities of the soft SUSY

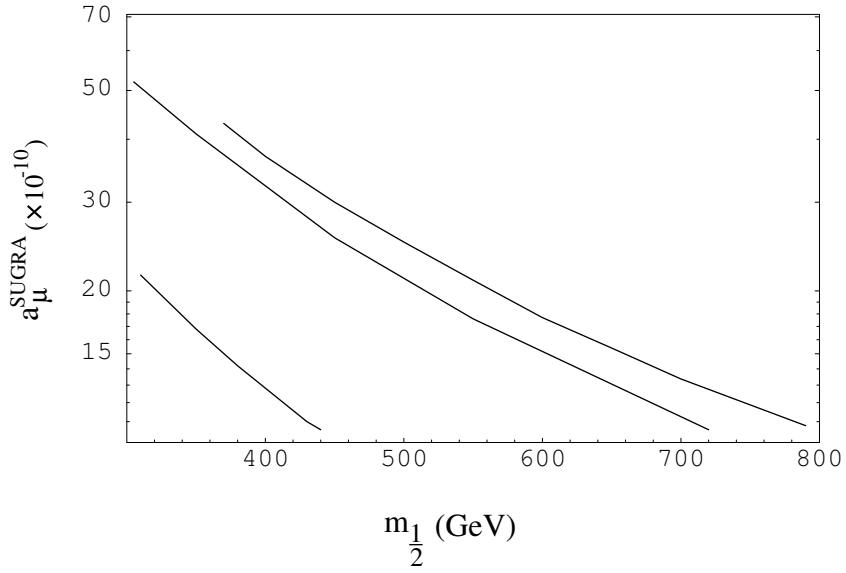

Fig. 5. mSUGRA contribution to a_μ as a function of $m_{1/2}$ for $A_0 = 0$, $\mu > 0$, for $\tan\beta = 10$, 30 and 40 (bottom to top).

breaking parameters in (2.6). For example, A reduction of μ^2 by properly shifting scalar masses from the universal value, m_0, increases the higgsino content of the neutralino, and thus increases the $\tilde{\chi}_1^0 - \tilde{\chi}_1^0 - Z$ coupling and opens a new region of allowed relic density at high $m_{1/2}$ and high $\tan\beta$ [59]. The lower bound of a_μ again eliminates large m_0 and $m_{1/2}$ region and ensures that the minimal neutralino-proton cross section remains detectable.

3. Discussion

The above discussion shows that for the mSUGRA model and it extensions with non-universalities the a_μ data, when combined with the m_h, $b \to s\gamma$ and relic density constraints have begun to greatly limit the SUSY parameter space. Thus the m_h and $b \to s\gamma$ constraints determine a lower bound on $m_{1/2}$ and hence an upper bound on $a_\mu^{\rm SUGRA}$, while the experimental lower bound on a_μ determines an upper bound on

Table I. Allowed ranges for SUSY masses in GeV for mSUGRA assuming 90% C. L. for a_μ for $A_0 = 0$.

$\tilde{\chi}_1^0$	$\tilde{\chi}_1^\pm$	$\tilde{g}$	$\tilde{\tau}_1$	$\tilde{e}_1$	$\tilde{u}_1$	$\tilde{t}_1$
(123-237)	(230-451)	(740-1350)	(134-264)	(145-366)	(660-1220)	(500-940)

$m_{1/2}$. The combined a_μ and m_h bound puts lower bound on $\tan\beta$ for a given value of A_0. This can be seen most clearly in Fig. 5, where the mSUGRA contribution to a_μ is plotted as a function of $m_{1/2}$ for $A_0 = 0$, $\tan\beta = 10$ (lower curve), $\tan\beta = 30$ (middle curve)and $\tan\beta = 40$ (upper curve). Further, most of the allowed $m_{1/2}$ region lies in the the $\tilde{\tau}_1 - \tilde{\chi}_1^0$ co-annihilation domain ($m_{1/2} \gtrsim 350$ GeV), and so from Fig. 4 one can see that m_0 is approximately determined in terms of $m_{1/2}$. In Fig. 5, the m_h bound determines the lower limit on $m_{1/2}$ for $\tan\beta$=10, while $b \to s\gamma$ determines it for $\tan\beta = 40$. Both are equally constraining for $\tan\beta$ =30. If we consider the 90% C. L. bound ($a_\mu > 21 \times 10^{-10}$) [64]), one finds for $A_0 = 0$ that $\tan\beta \geq 10$, and for $\tan\beta \leq 40$ that $m_{1/2} = (290 - 550)$ GeV, and $m_0 = (70 - 300)$ GeV. This greatly constrains SUSY particle spectrum expected at accelerators, as can be seen in Table I. Thus at the 90% C.L. bound on a_μ only the $\tilde{\tau}_1$ and $\tilde{e}_1$ would possibly be within the reach of a 500 GeV NLC (and very marginally the $\tilde{\chi}_1^\pm$), while all the SUSY particles would be accessible to the LHC.

Another interesting features of Fig. 5 is that mSUGRA can no longer accommodate large values of $a_\mu^{\rm SUGRA}$. If the future data should require a value significantly larger than 40×10^{-10}, this would be a signal for the existence of non-universal soft breaking. From (3.11) one sees that one can increase a_μ by reducing μ, and as explained, this might be accomplished by non-universal soft breaking of the scalar masses (and also from non-universal gaugino masses at M_G.) Thus the $g_\mu - 2$ ex-

periment may give us significant insight into the nature of physics beyond the GUT scale.

CHAPTER IV

$B^0 \to \phi K_S$ IN SUGRA MODELS WITH CP VIOLATIONS*

The SM is described by a locally Lorentz invariant Lagrangian. By virtue of the CPT theorem, the SM is then invariant under a combined C (charge conjugation), P (Parity) and T (time reversal) transformation. Experimentally CPT violation has not yet been observed [1], but C, P and CP violations have been found in nature. Although there is no direct experimental evidence of T violation, the CPT theorem implies that T symmetry is also not a good symmetry if nature is described by a locally Lorentz invariant theory, e.g. the SM.

In the SM, parity and charge conjugation symmetries are maximally violated due to the $V-A$ structure of the electroweak interaction. However, if the CKM phase δ (see appendix A) were zero, CP would be invariant in the SM. Therefore, observed CP violations imply a non-zero δ which can be extracted from CP violating processes dominated by the SM contributions. The current fit of the experimental data to the SM gives $\delta = 59^\circ \pm 13^\circ$ [1]. The CP violating nature of the CKM matrix can be seen in the unitarity triangle as follows. Since $V^\dagger_{\rm CKM} V_{\rm CKM} = {\rm I}$ (where I is the unit matrix), one has

$$V^*_{ub}V_{ud} + V^*_{cb}V_{cd} + V^*_{tb}V_{td} = 0 \tag{4.1}$$

The unitarity triangle can then be constructed in the complex plane as shown in

*Tables and figures presented in this chapter are reprinted with permission from "$B^0 \to \phi K_S$ in SUGRA Models with CP Violations" by R. Arnowitt, B. Dutta, B. Hu, 2003, Phys. Rev. D 68, 075008 (10 Pages). Copyright 2003 by the American Physical Society.

[1]It has been suggested that the current neutrino data, including the LSND (the Liquid Scintillating Neutrino Detector) data, might imply a breakdown of the CPT invariance. (For a review, see [65].)

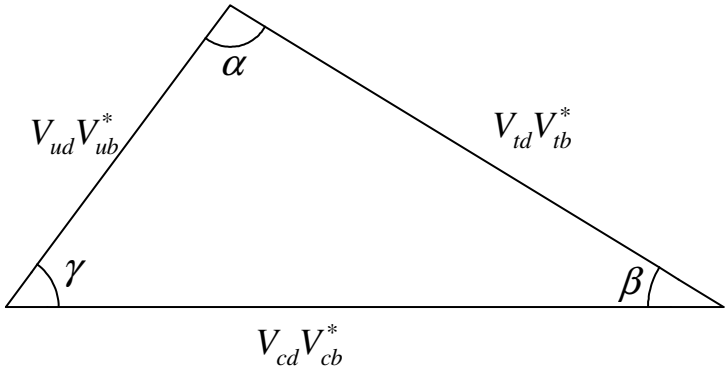

Fig. 6. The unitary triangle representation of (4.1).

Fig. 6. All the CKM elements, including the three angles of the unitarity triangle, can be measured experimentally, especially in B decays (a summary of the current experimental status can be found in [66]). It is then possible to test the validity of the SM by examining its consistency with the experimental data. Although most experiments are in agreement with the SM predictions, a possible deviation has been found in the $B^0 \to \phi K_S$ decay. This deviation has been discussed by many authors (see [67] and references therein) in the SUSY framework, especially in the minimal supersymmetric standard model (MSSM) by employing the mass insertion method [30]. Although these analyses can provide useful constraints on some off-diagonal terms of the squark mass matrices, as explained in Chapter 2, it is certainly worthwhile to investigate this problem in the context of grand unified models, especially the R-parity conserved SUGRA models which can also provide a natural explanation to the dark matter problem. Here we will examine the apparent deviation from the SM found in $B \to \phi K$ decays in the context of SUGRA models including mSUGRA and models with non-universalities. We also impose all other relevant experimental constraints.

We begin by giving a brief description of the $B \to \phi K$ decays, the current exper-

imental status of their CP asymmetries and branching ratios (BRs) and the discrepancy found in the $B^0 \to \phi K_S$ decay. We also briefly discuss the QCD factorization technique used in this work. (More details are given in appendices.)

1. CP asymmetry of $B \to \phi K$ decays

The time dependent CP asymmetry of $B \to \phi K_S$ is described by (see Appendix B):

$$\begin{aligned} \mathcal{A}_{\Phi K_S}(t) &\equiv \frac{\Gamma(\overline{B}^0_{\rm phys}(t) \to \phi K_S) - \Gamma(B^0_{\rm phys}(t) \to \phi K_S)}{\Gamma(\overline{B}^0_{\rm phys}(t) \to \phi K_S) + \Gamma(B^0_{\rm phys}(t) \to \phi K_S)} \\ &= -C_{\phi K_S} \cos(\Delta m_B t) + S_{\phi K_S} \sin(\Delta m_B t) \end{aligned} \tag{4.2}$$

where $S_{\phi K_S}$ and $C_{\phi K_S}$ are given by

$$S_{\phi K_S} = \frac{2\,{\rm Im}\lambda_{\phi K_S}}{1+|\lambda_{\phi K_S}|^2}\,, \quad C_{\phi K_S} = \frac{1-|\lambda_{\phi K_S}|^2}{1+|\lambda_{\phi K_S}|^2}\,, \tag{4.3}$$

and $\lambda_{\phi K_S}$ can be written in terms of decay amplitudes:

$$\lambda_{\phi K_S} = -e^{-2i\beta} \frac{\overline{\mathcal{A}}(\overline{B}^0 \to \phi K_S)}{\mathcal{A}(B^0 \to \phi K_S)}\,. \tag{4.4}$$

In principal, the β in (4.4) should include the SUSY contributions to the $B_d - \overline{B}_d$ mixing, which, however, are found to be small. Hence we will use the standard definition for β:

$$\beta \equiv \arg\left(\frac{V_{cd}V_{cb}^\star}{V_{td}V_{tb}^\star}\right). \tag{4.5}$$

This definition is invariant under quark field rephasing, as are the other physical observables.

Within the SM, $\sin 2\beta$ can be measured by $S_{J/\Psi K_S}$ in the $B \to J/\Psi K_S$ decay (which is a tree level process). The current world average is

$$S_{J/\Psi K_S} = 0.734 \pm 0.055 \tag{4.6}$$

which is in excellent agreement with Buras' SM evaluation, $\sin 2\beta = 0.715^{+0.055}_{-0.045}$ from the CKM matrix [68] which does not make use of the $B \to J/\Psi K_S$ data. Since $B \to J/\Psi K_S$ decay is dominated by the SM tree level contribution, we expect that in our analysis the new physics will not affect the SM prediction for $\sin 2\beta$ from $B \to J/\Psi K_S$. As a consequence, we further assume that the current SM fit for the CKM matrix will not be affected by models discussed here.

The SM also predicts that the CP asymmetries of $B^0 \to \phi K_S$ and $B \to J/\Psi K_S$ should measure the same $\sin 2\beta$ with negligible $O(\lambda^2)$ corrections [69]. On the other hand, the BaBaR and Belle measurements [70, 71, 72, 73] show a 2.7σ disagreement between $S_{\phi K_S}$ and $S_{J/\Psi K_S}$ [2]

$$S_{\phi K_S} = -0.38 \pm 0.41 \ . \tag{4.7}$$

In addition, the branching ratios (BRs) and the direct CP asymmetries of both the charged and neutral modes of $B \to \phi K$ have also been measured [70, 71, 72, 73][3]:

$$\begin{aligned} \mathrm{Br}[B^0 \to \phi K_S] &= (8.0 \pm 1.3) \times 10^{-6}, \\ \mathrm{Br}[B^+ \to \phi K^+] &= (10.9 \pm 1.0) \times 10^{-6}, \qquad (4.8) \\ C_{\phi K_S} &= -0.19 \pm 0.30, \\ \mathcal{A}_{CP}(B^+ \to \phi K^+) &= (3.9 \pm 8.8 \pm 1.1).\% \qquad (4.9) \end{aligned}$$

Where $\mathcal{A}_{CP}$ is the CP asymmetry of the charged $B \to \phi K$ decay defined as

$$\mathcal{A}_{CP} \equiv \frac{\Gamma(B^- \to \phi K^-) - \Gamma(B^+ \to \phi K^+)}{\Gamma(B^- \to \phi K^-) + \Gamma(B^+ \to \phi K^+)} = \frac{|\lambda_{\phi K^\mp}|^2 - 1}{|\lambda_{\phi K^\mp}|^2 + 1} \tag{4.10}$$

[2] After this work was done new data from Belle [9] gave a value of $S_{\phi K_S} = -0.96 \pm 0.5^{+0.09}_{-0.11}$ (a 3.5σ deviation from the Standard Model) and new data from BaBar [74] gave $S_{\phi K_S} = +0.47 \pm 0.34$. Belle and BaBar would then disagree by more than 2σ and if one averages the new values one obtains [75] $S_{\phi K_S} = 0.02 \pm 0.29$ which is 2.5σ from the Standard Model [76].

[3] Our average of $\mathrm{Br}[B^+ \to \phi K^+]$ only includes BaBar and Belle since CLEO [77] is 2.3σ away. $\mathrm{Br}[B^+ \to \phi K^+]$ would become $(9.4 \pm 0.9) \times 10^{-6}$ if CLEO is included.

with

$$\lambda_{\phi K^{\mp}} = \frac{\overline{A}(B^- \to \phi K^-)}{A(B^+ \to \phi K^+)}. \tag{4.11}$$

In general, any model should explain all these data. In particular, the relatively small uncertainties in the BRs of $B^+ \to \phi K^+$ and $B^0 \to \phi K_S$ need to be considered in the analysis since they are highly correlated and both are based on the $b \to s$ transition. In the SM, $\mathcal{A}_{CP}(B^+ \to \phi K^+)$ is small and agrees with (4.9). So this direct CP asymmetry result plays an important role in constraining the new physics contribution which might explain the discrepancy between $S_{\phi K_S}$ and $S_{J/\Psi K_S}$.

2. Decay amplitudes

From the above discussion, it is clear that our theoretical predictions for the experimental observables, e.g. $S_{\phi K_S}$, $C_{\phi K_S}$ and $\mathcal{A}_{\phi K^{\mp}}$, depend on the evaluation of decay amplitudes. The most difficult part is the evaluation of the matrix elements of related operators in the effective Hamiltonian between initial and final hadronic states, e.g. $|B\rangle$ and $\langle \phi K|$ in the case of $B \to \phi K$ decays. There are many ways of doing this calculation. Here we adopt the newly developed QCD improved factorization (BBNS approach) [78, 79, 80] which provides a systematic way to calculate the matrix elements of a large class of B decays with significant improvements over the old factorization approach (naive factorization). It allows a QCD calculation of "non-factorizable" contributions and model independent predictions for strong phases which are important in the theoretical evaluation of the direct CP asymmetries of B decays, e.g. for $B^- \to \phi K^-$. Recently Du et al. [81, 82, 83] have published an improved calculation of $B \to PV$ decays. We followed here their calculational techniques [81] which are based on the original work [78, 79, 80] of Beneke, et al.

Before proceeding on, we would like to make one comment. While the BBNS

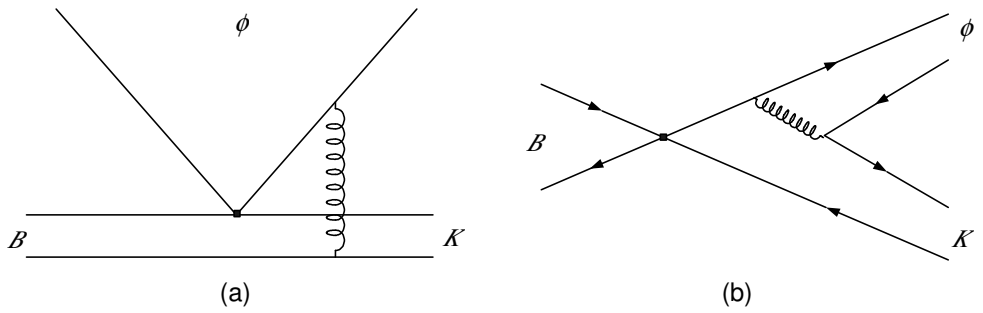

Fig. 7. Hard spectator scattering diagram (a) and weak annihilation diagram (b). In (a) the gluon can connect the spectator with either ϕ quark and in (b) the gluon can originate from any B quark or K quark.

approach is an important advance in calculating B decays, it is not completely model independent. In the BBNS approach the hard gluon (H) and annihilation (A) diagrams (see Fig. 7) contain infrared divergences which are parameterized by an amplitude $\rho_{H,A}$ (with $\rho_{H,A} \leq 1$) and a phase $\phi_{H,A}$. (More details can be found in [78, 79, 80] and [81].) If the effects of these terms are small, the theoretical predictions are well defined. However, if these terms are large or dominant, the theory becomes suspect. We will see below that $S_{\phi K_s}$ is essentially independent of the infrared divergent terms, though the branching ratios can become sensitive to ρ_A and ϕ_A.

The Effective Hamiltonian for $B \to \phi K$ in the SM is:

$$\begin{aligned} \mathcal{H}_{eff} &= \frac{G_F}{\sqrt{2}} \sum_{p=u,\,c} V_{pb} V_{ps}^{\star} \Big[C_1 O_1^p + C_2 O_2^p + \sum_{k=3}^{10} C_k(\mu) O_k(\mu) \\ &\quad + C_{7\gamma} O_{7\gamma} + C_{8g} O_{8g} \Big] + \text{h.c.} \end{aligned} \tag{4.12}$$

where $Q_{1,2}^p$ are tree operators, $Q_{3,\ldots,6}$, QCD penguin operators, $Q_{7,\ldots,10}$, electroweak penguin operators, and $Q_{7\gamma}$ and Q_{8g}, the electromagnetic and chromomagnetic dipole operators. The explicit forms of O_i's are given by

$$Q_1^p = (\bar{p}b)_{V-A}(\bar{s}p)_{V-A}\,, \qquad Q_2^p = (\bar{p}_i b_j)_{V-A}(\bar{s}_j p_i)_{V-A}\,,$$

$$
\begin{aligned}
Q_3 &= (\bar{s}b)_{V-A}(\bar{q}q)_{V-A}\,, & Q_4 &= (\bar{s}_i b_j)_{V-A}(\bar{q}_j q_i)_{V-A}\,,\\
Q_5 &= (\bar{s}b)_{V-A}(\bar{q}q)_{V+A}\,, & Q_6 &= (\bar{s}_i b_j)_{V-A}(\bar{q}_j q_i)_{V+A}\,,\\
Q_7 &= (\bar{s}b)_{V-A}\tfrac{3}{2}e_q(\bar{q}q)_{V+A}\,, & Q_8 &= (\bar{s}_i b_j)_{V-A}\tfrac{3}{2}e_q(\bar{q}_j q_i)_{V+A}\,,\\
Q_9 &= (\bar{s}b)_{V-A}\tfrac{3}{2}e_q(\bar{q}q)_{V-A}\,, & Q_{10} &= (\bar{s}_i b_j)_{V-A}\tfrac{3}{2}e_q(\bar{q}_j q_i)_{V-A}\,,\\
Q_{7\gamma} &= \frac{-e}{8\pi^2}\, m_b\, \bar{s}\sigma_{\mu\nu}(1+\gamma_5)F^{\mu\nu}b\,,\\
Q_{8g} &= \frac{-g_s}{8\pi^2}\, m_b\, \bar{s}\sigma_{\mu\nu}(1+\gamma_5)G^{\mu\nu}b\,,
\end{aligned}
\tag{4.13}
$$

where $V \pm A = \gamma_\mu(1 \pm \gamma_5)$, i, j are color indices and a summation over $q = u, d, s, c, b$ is implied. The Wilson coefficients $C_i(\mu)$ in (4.12) can be obtained by running the RGEs from the weak scale down to scale μ. The SUSY contributions will bring in new operators $\tilde{O}_i$'s which can be obtained by changing $L \leftrightarrow R$ in the SM operators. We use $\tilde{C}_i$ to denote the Wilson coefficient of $\tilde{O}_i$.

Using the above Hamiltonian the amplitude of $B \to \phi K$ is:

$$\mathcal{A}(B \to \phi K) = \mathcal{A}^f(B \to \phi K) + \mathcal{A}^a(B \to \phi K) \tag{4.14}$$

where $\mathcal{A}^f$ are the factorized amplitudes which can be written as

$$\mathcal{A}^f(B \to \phi K) = \frac{G_F}{\sqrt{2}} \sum_{p=u,\,c} \sum_i V_{pb}V_{ps}^\star a_i^p \langle \phi K|O_i|B\rangle_f\ , \tag{4.15}$$

and $\mathcal{A}^a$ is the weak annihilation decay amplitudes [81]:

$$\mathcal{A}^a(B \to \phi K) = \frac{G_F}{\sqrt{2}} f_B f_\phi f_K \sum V_{pb}V_{ps}^\star b_i. \tag{4.16}$$

The matrix elements $\langle \phi K|O_i|B\rangle_f$ in (4.15) are the factorized hadronic matrix elements [84]. a_i's and b_i's contain the Wilson coefficients. Explicit expressions for them, as well as for $\mathcal{A}^a(B \to \phi K)$, can be found in [80] and [81].

One comment is that the decay amplitudes are calculated at scale $\mu \sim m_b$ where only QCD effects are relevant. Our SUSY contributions are hidden in the Wilson coefficients. The main idea is still that of the effective field theory: all the Wilson

coefficients are first calculated at the weak scale by integrating out heavy particles including the heavy gauge bosons, the top quark and the superpartners (or any relevant non-SM particles), and then run down to the scale $\mu \sim m_b$ via the RGEs of the effective theory [85].

3. $B \to \phi K$ decays in the Standard Model

We first discuss the $B \to \phi K$ decays in the SM. The largest theoretical uncertainties in this calculation come from weak annihilation diagrams which mostly depend on the divergent end-point integrals X_A parameterized in the form [80, 81]

$$X_A = (1 + \rho_A e^{i\phi_A}) \ln \frac{m_B}{\Lambda_h}, \quad \Lambda_h = \Lambda_{QCD}, \quad \rho_A \leq 1. \tag{4.17}$$

Hard spectator processes contain similar integrals X_H which are parameterized in the same way with ρ_A and ϕ_A in (4.17) being replaced by ρ_H and ϕ_H. However, uncertainties from the hard spectator calculation are much smaller than those from the weak annihilation for this decay, so we will mainly concentrate on the later. These weak annihilation contributions depend also on the strange quark mass, m_s, through the chirally enhanced factor κ_χ [80]:

$$\kappa_\chi = \frac{2m_K^2}{m_b(m_s + m_q)} \tag{4.18}$$

where m_q is m_d or m_u.

In Fig. 8 we show the dependence of the branching ratio of $B^- \to \phi K^-$ mode on ϕ_A and m_s for $\rho_A = 1$. Fig. 9 shows the dependence of the BR on ρ_A for $\phi_A = 0$. Similar graphs can be obtained for $B^0 \to \phi K^0$. Since in the SM the direct CP asymmetry of charged $B \to \phi K$ decay (i.e. $\mathcal{A}_{CP}$ defined by (4.10)) is small, we can compare $\mathrm{Br}[B^- \to \phi K^-]$ with the experimental measurement of $\mathrm{Br}[B^+ \to \phi K^+]$ given in (4.8).

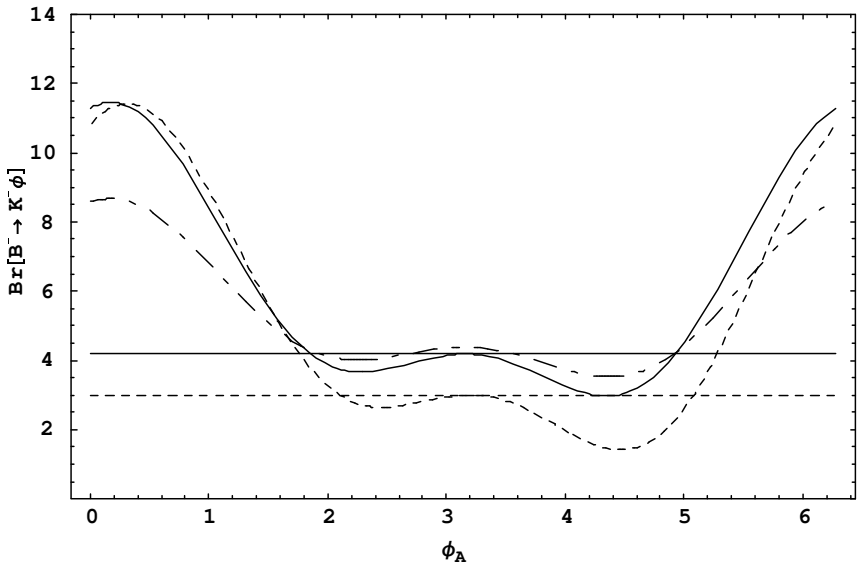

Fig. 8. Branching ratio of $B^- \to \phi K^-$ at $\rho_A = 1$. The solid curve corresponds to $\mu = m_b$, dashed curve for $\mu = 2.5\,\mathrm{GeV}$ with $m_s(2\,\mathrm{GeV}) = 96\,\mathrm{MeV}$ and the dot-dashed curve for $\mu = m_b$ with $m_s(2\,\mathrm{GeV}) = 150\,\mathrm{MeV}$. The two straight lines correspond to the cases without weak annihilation.

Before we discuss the graphs, we first list our parameters: $\rho_H = 1$ and $\phi_H = -68^\circ$ for the X_H defined as (4.17), $f_B = 180\,\mathrm{MeV}$, $f_\phi = 233\,\mathrm{MeV}$ and $f_K = 160\,\mathrm{MeV}$ for the decay constants of the B, ϕ and K mesons and $F^{BK} = 0.34$ for the $B \to K$ form factor [84, 86, 87, 88, 89]. The CKM matrix elements can be obtained through the Wolfenstein parameterization [90]

$$V_{\mathrm{CKM}} \equiv \begin{pmatrix} 1-\lambda^2/2 & \lambda & A\lambda^3(\rho - i\eta) \\ -\lambda & 1-\lambda^2/2 & A\lambda^2 \\ A\lambda^3(1-\rho-i\eta) & -A\lambda^2 & 1 \end{pmatrix} + \mathcal{O}(\lambda^4). \tag{4.19}$$

with $A = 0.819$, $\lambda = 0.2237$, $\rho = 0.224$ and $\eta = 0.324$ [91, 92]. The integral $\int_0^1 (\Phi_B(\xi)/\xi) d\xi = m_B/\lambda_B$, where Φ_B is the B meson light-cone distribution amplitude, is parameterized by $\lambda_B = (0.35 \pm 0.15)$ GeV [80]. For $\mu = 2.5\,\mathrm{GeV}$ we use $\lambda_B = 0.2\,\mathrm{GeV}$, and for $\mu = m_b$ we use $\lambda_B = 0.47\,\mathrm{GeV}$. In addition, we always use asymptotic

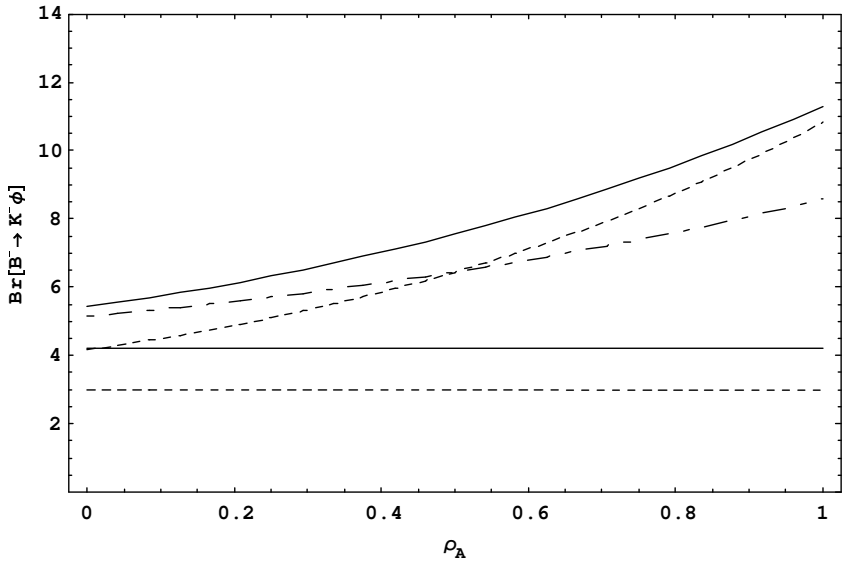

Fig. 9. Branching ratio of $B^- \to \phi K^-$ at $\phi_A = 0$. The solid curve corresponds to $\mu = m_b$, dashed curve for $\mu = 2.5\,\mathrm{GeV}$ with $m_s(2\,\mathrm{GeV}) = 96\,\mathrm{MeV}$ and the dot-dashed curve for $\mu = m_b$ with $m_s(2\,\mathrm{GeV}) = 150\,\mathrm{MeV}$. The two straight lines correspond to the cases without weak annihilation.

forms of the meson light-cone distribution amplitudes [80, 81]. If not mentioned, we will use the above parameters in later calculations.

In both figures, we give results for two different scales and two different m_s values, i.e., $\mu = m_b$ by solid lines ($m_s(2\,\mathrm{GeV}) = 96\,\mathrm{MeV}$) and the dot-dashed lines ($m_s(2\,\mathrm{GeV}) = 150\,\mathrm{MeV}$) and $\mu = 2.5\,\mathrm{GeV}$ by dashed lines ($m_s(2\,\mathrm{GeV}) = 96\,\mathrm{MeV}$). One can see that the scale dependence is not significant. The straight lines correspond to the branching ratios neglecting the weak annihilation contribution. Comparing Figs 8 and 9, we see that a large branching ratio comparable to the experimental value is obtained only in the region $\rho_A \simeq 1$ and $\phi_A \simeq 0(\text{or } 2\pi)$. However, in this region the weak annihilation diagrams dominate the branching ratio and thus the theory is most suspect. In the remaining part of the parameter space, where the weak annihilation effects are small and the theory is presumably reliable (which is

the most of the parameter space), the SM prediction of the branching ratio is small, about 3σ below the experimental value. We conclude therefore that where the theory is reliable the SM is in significant disagreement with the experimental value of the $\mathrm{Br}[B^+ \to \phi K^+]$, and in order to obtain a SM value in accord with the experiment one must use parameters where the theory is least reliable. A similar result holds for the $\mathrm{Br}[B^0 \to \phi K_s]$. Here theory predicts a branching ratio about 10% smaller than for $B^+ \to \phi K^+$ (in accord with the experimental values of (4.8)) but again the SM can achieve this only in the region where the weak annihilation processes dominate.

The dot-dashed line, in Fig. 8, corresponds to a larger value of m_s and we see that the BR is very sensitive to m_s only in the large annihilation region. The region with sufficiently large annihilation to accommodate the data decreases as m_s increases, since the annihilation amplitude then decreases, as can be seen from (4.18).

As explained in the previous section, the SM predictions for $S_{\phi K_S}$ and $S_{J/\Psi K_S}$ already have a large discrepancy. The analysis in this section shows that the SM also cannot account for the branching ratios, further increasing the need for new physics. In the next two sections we will discuss this problem in the framework of SUGRA models. We first show in the next section that the mSUGRA model suffers from the same problems as the SM. We then extend mSUGRA by adding non-universal A terms and show that the current experimental results can be well accommodated.

4. mSUGRA

As shown in Chapter II, the SUGRA model at the GUT scale can be described by its superpotential and soft-breaking terms:

$$W_Y = Y^{(u)} q_L H_2 u_R + Y^{(d)} q_L H_1 d_R + Y^{(e)} l_L H_1 e_R + \mu H_1 H_2$$

$$\mathcal{L}_{soft} = -\sum_i m_i^2|\phi_i|^2 - \frac{1}{2}\sum_\alpha m_\alpha \bar{\lambda}_\alpha \lambda_\alpha - \Big(B\mu H_1 H_2 + \big(A^U q_L H_2 u_R + A^D q_L H_1 d_R + A^L l_L H_1 e_R\big) + \text{h.c.}\Big). \tag{4.20}$$

where m_i's denote scalar masses. In the minimal picture, the mSUGRA model contains a universal scalar mass m_0, a universal gaugino mass $m_{1/2}$ and the universal cubic scalar A terms:

$$m_i^2 = m_0^2, \quad m_\alpha = m_{1/2}, \quad A^{U,D,L} = A_0 Y^{(u,d,e)}. \tag{4.21}$$

This model contains four free parameters and a sign: m_0, $m_{1/2}$, A_0, $\tan\beta = \langle H_2\rangle/\langle H_1\rangle$ and the sign of μ.

The mSUGRA model discussed in this section is the usual mSUGRA model extended by allowing non-zero CP violating phases which are necessary for the discussion of CP violating processes, e.g. $B \to \phi K$ decays in this work. In general, the parameters $m_{1/2}$, A_0 and μ can be complex and their phases can be $O(1)$. In order to accommodate the experimental bounds on the electron and neutron EDMs without fine tuning phases we extend mSUGRA by allowing the gaugino masses at M_G to have arbitrary phases [41, 42]. Thus the SUSY parameters with phases at the GUT scale are

$$m_\alpha = |m_{1/2}|\,\exp(i\phi_\alpha), \quad A_0 = |A_0|\,\exp(i\alpha_A) \quad \text{and} \quad \mu = |\mu|\,\exp(i\phi_\mu) \tag{4.22}$$

where $\alpha = 1, 2, 3$. However, by a phase transfomation we can set one of the gaugino phases to zero and we choose $\phi_2 = 0$ (see, e.g. [13] for a discussion on phase reparameterization). Therefore, we are left with four phases. The EDMs of the electron and neutron can now allow the existence of large phases in the theory [93, 94, 95, 41, 42]. In our work, we use $O(1)$ phases satisfying the EDM bounds given in (2.21).

We evolve the above parameters from the GUT scale down to the weak scale using full matrix RGEs. Since the $b \to s$ transition is a generation mixing process, it

Table II. $S_{\phi K_S}$ at $\tan\beta = 10$ and 40 in mSUGRA.

$\tan\beta$	10				40			
$\lvert A_0\rvert$	800	600	400	0	800	600	400	0
$m_{1/2} = 400$	0.74	0.74	0.73	0.73	0.71	0.70	0.70	0.69
$m_{1/2} = 500$	0.74	0.74	0.74	0.74	0.72	0.72	0.72	0.71

is necessary to use the full 6×6 matrix form of squark mass matrices in the calculation. We also include the one loop correction to bottom quark mass from SUSY [29], which is important in the calculation of SUSY contributions to the Wilson coefficients of the operator $O_{7\gamma}$ and O_{8g} and consequently affects the calculations of $B \to X_s\gamma$ and $B \to \phi K$ decays.

We now discuss the mSUGRA predictions on $B \to \phi K$ decays. Again let us first mention the values of the parameters used in our calculation. We use $\rho_{A,H} = 1$, $\phi_{A,H} = -68^\circ$, $m_s(2\,\mathrm{GeV}) = 122.5\,\mathrm{MeV}$ and a CKM fit giving $\sin 2\beta = 0.73$ and $\gamma = 59^\circ$. (If we increase γ, the BR decreases, e.g. for $\gamma = 79^\circ$, the SM BR decreases by $\sim 2\%$.) The SM braching ratio based on the same set of parameters is 4.72×10^{-6} and the weak annihilation contribution is small (~ 10 %).

In Table II, we give the numerical results for two different values of the mSUGRA parameter $\tan\beta$ cases i.e. $\tan\beta = 40$ and 10 and for different $m_{1/2}$ and A_0 in the small weak annihilation case. The values given in Table II are the minimum that can be reached subject to all other experimental constraints. For simplicity, we set $\alpha_A = \pi$ in the calculation of Table II. We use large phases for other parameters but still satisfy the EDM constrains. For example, for $m_{1/2} = 400$ GeV and $A_0 = 800$ GeV with $\tan\beta = 40$, we find that $\phi_1 = 70^\circ$, $\phi_3 = 33^\circ$ and $\phi_\mu = -13^\circ$ (at the weak scale) satisfy the EDM constraints (for reasons discussed in detail in [41, 42]).

The phase α_A has a very small effect on $S_{\phi K_S}$ and this effect becomes smaller as the magnitude of A decreases. Thus a different value of α_A, in the above fit, can change $S_{\phi K_S}$ by $\pm 4\%$ for $A_0 = 800$ GeV. This change is even smaller for smaller A_0, e.g. for $A_0 = 200$ GeV, the change in $S_{\phi K_S}$ is less than 2%. The values of m_0, for different $m_{1/2}$ and A_0, are chosen such that the relic density constraint is satisfied. As shown in Fig 4, the allowed range of m_0 for a given $m_{1/2}$ is very small and thus any m_0 in the allowed range can be used since the processes considered here are not sensetive to the value of m_0. We also satisfy the $\mathrm{Br}[b \to s + \gamma]$ constraint and the Higgs mass constraint.

It can be seen from Table II that the $S_{\phi K_S}$ values in mSUGRA differ only slightly from the SM prediction which is $\sin 2\beta$ evaluated using just the CKM phase. The branching ratios of $B \to \phi K$ decays also do not differ much from the SM prediction. Even if one went to the large weak annihilation region to accommodate the large branching ratios, $S_{\phi K_S}$ would still be similar to the numbers in Table II. Therefore, mSUGRA can not explain the large BR and the 2.7σ difference between the $S_{\phi K_S}$ and the $S_{J/\Psi K_S}$ experimental results. The reason is that, in mSUGRA, the only flavor violating source is in the CKM matrix, which cannot provide enough flavor violation needed for the $b \to s$ transition in $B \to \phi K$ decays. In the next section, we will search for the minimal extension of mSUGRA that can solve both the BR and CP problems of $B \to \phi K$ decays.

5. SUGRA model with Non-universal A terms

In the last section, we showed that mSUGRA contributions to $B \to \phi K$ decays are negligible and thus mSUGRA needs to be extended if it is to explain the experimental results of $B \to \phi K$ decays. It is obvious that some non-universal soft breaking terms

which can contribute to the $b \to s$ transition are necessary. There are two ways of enhancing the mixing between the second and the third generation: one can have non universal terms in the squark mass matrices or in the $A^{U,D}$ matrices of (4.20). However, in a GUT model, at least the Standard Model gauge group must hold at M_G and hence the only squark m^2_{23} that can occur is either left-left or right-right coupling. As discussed in [96], such non-universal terms produce only small effects on $B \to \phi K$ decays. Thus we are led to models with left-right mixing which can occur in the $A^{U,D}$ matrices as the simplest possible non-universal term relevant to $B \to \phi K$ decays. In this work then, we choose a model with non-zero (2,3) elements in the trilinear coupling A terms of (4.20) to enhance the left-right mixing of the second and the third generation. The A terms with non-zero 23 elements can be written as

$$A^{U,D} = A_0 Y^{(u,d)} + \Delta A^{U,D} \tag{4.23}$$

where $\Delta A^{U,D}$ are 3×3 complex matrices and $\Delta A^{U,D}_{ij} = |\Delta A^{U,D}_{ij}| \exp(i\phi^{U,D}_{ij})$. When $\Delta A^{U,D} = 0$, mSUGRA is recovered. For simplicity, we discuss first the case of non-zero ΔA^D_{23} and non-zero ΔA^D_{32} for $\tan\beta = 10$ and 40. In both cases, all other entries in $\Delta A^{(u,d)}$ are set to zero. The other parameters are same as in the mSUGRA case. We also set the phases such that the EDM constraints are obeyed. At the GUT scale, we use a diagonal Yukawa texture for $Y^{(u)}$, while $Y^{(d)}$ is constructed as $VY^{(d)}_d$ where V is the CKM matrix and $Y^{(d)}_d$ is the diagonalized matrix of the down type Yukawa. The phenomenological requirements for the Yukawa matrices are that they produce the correct quark masses and the correct CKM matrix. Any other Yukawa texture which satisfies the same requirements can be obtained through a unitary rotation. Therefore, our results can be recovered with other Yukawa textures if our A terms are rotated along with the Yukawas.

In the calculations of decay amplitudes, we will use QCD parameters for the small weak annihilation region (see the last section) where the theory is reliable. In general it is possible that (see [81] for the calculational details of weak annihilation) the new physics can change the behavior of annihilation contributions so that the relevant Wilson coefficients can be reduced or increased significantly. However, in our case with non-zero $\Delta A^{U,D}_{23,32}$ terms, the SUSY contribution mainly affects the Wilson coefficients $C_{8g(7\gamma)}$ (possibly also $\tilde{C}_{8g(7\gamma)}$) and these coefficients will not change the annihilation contributions compared to what we have in the SM calculation and thus our previous conclusion about the annihilation terms still holds.

5.1. Case I: $|\Delta A^D_{23}| = |\Delta A^D_{32}|$ *and* $\phi^D_{23} \neq \phi^D_{32}$

We show our results for $|\Delta A^D_{23}| = |\Delta A^D_{32}|$ but $\phi^D_{23} \neq \phi^D_{32}$ with $\tan\beta = 10$ in Table III. We note that $|\Delta A^D_{23(32)}|$ is an increasing function of $m_{1/2}$. The phases ϕ^D_{23} and ϕ^D_{32} are approximately -30° and $(75 \sim 115)^\circ$, respectively. The other SUSY phases are: $\phi_1 \sim 22^\circ$, $\phi_3 \sim 31^\circ$ and $\phi_\mu \sim -11^\circ$. In addition, as mentioned above, the phase of A_0, i.e. α_A, is set to be π.

The $\mathrm{Br}[B^- \to \phi K^-]$ is $\sim 10 \times 10^{-6}$ in the parameter space of Table III. We satisfy all other experiment constraints. We see that SUGRA models can explain the

Table III. $S_{\phi K_S}$ at $\tan\beta = 10$ with non-zero A^D_{23} and A^D_{32}.

$\lvert A_0\rvert$	800	600	400	0	$\lvert\Delta A^D_{23(32)}\rvert$
$m_{1/2} = 300$	-0.50	-0.49	-0.47	-0.43	~ 50
$m_{1/2} = 400$	-0.43	-0.40	-0.38	-0.36	~ 110
$m_{1/2} = 500$	-0.46	-0.46	-0.44	-0.31	~ 200
$m_{1/2} = 600$	-0.15	-0.13	-0.04	0.05	~ 280

large BR and $S_{\phi K_S}$ of the $B \to \phi K$ decay modes even in the small annihilation region. Comparing with (4.7), one sees that the values of $S_{\phi K_S}$ in the Table are within 1σ range of the experimental measurement. Reducing the Br$[B^- \to \phi K^-]$ allows one to increase $S_{\phi K_s}$. For example, for $A_0 = 0$ and $m_{1/2} = 600$ GeV, by adjusting ϕ^D_{32}, $S_{\phi K_s}$ can be reduced to -0.05 with Br$[B^- \to \phi K^-] \sim 9 \times 10^{-6}$. In Table IV we show the direct CP asymmetries of the $B^- \to \phi K^-$ decay, i.e. $\mathcal{A}_{\phi K^\mp}$, using the same parameters as Table III. The CP asymmetry is around $-(2 \sim 3)\%$ and agrees with the experimental result shown in Eq.(4.9). This prediction depends on the choice of $\phi_{A,H}$ in Eq.(4.17). For example, if we use $\phi_{A,H} = 28^\circ$, we generate a large $\mathcal{A}_{\phi K^\mp} \sim 27\%$. We find that there exists a reasonably large range of $\phi_{A,H}$ where we can satisfy the current bound on $\mathcal{A}_{\phi K^\mp}$. For example, at $m_{1/2} = 300$ GeV and $A_0 = 800$ GeV where the SUSY contribution is the largest, we find that $\mathcal{A}_{\phi K^\mp}$ varies from 9% to -4% when $\phi_{A,H}$ varies from -100° to -50° (for simplicity, we set $\phi_A = \phi_H$). In addition, since the annihilation contribution is small in that range, we find that the branching ratio is around $(9.5 \sim 11) \times 10^{-6}$. The CP asymmetry of $b \to s\gamma$ is ∼1-3%. The present experimental errors for $C_{\phi K_S}$ are still large. For this model, $C_{\phi K_S} \sim -\mathcal{A}_{\phi K^\mp}$, which may be tested by future data.

Table IV. $\mathcal{A}_{b\to s+\gamma} \times 10^2$ (left) and $\mathcal{A}_{\phi K^\mp} \times 10^2$ (right) at $\tan\beta = 10$ with non-zero A^D_{23} and A^D_{32}.

$\lvert A_0\rvert$	800		600		400		0	
$m_{1/2} = 300$	1.2	−3.7	1.4	−3.6	1.7	−3.6	2.2	−3.5
$m_{1/2} = 400$	1.9	−3.5	2.0	−3.4	2.2	−3.3	2.3	−3.3
$m_{1/2} = 500$	2.6	−3.5	2.6	−3.6	2.5	−3.5	2.4	−3.2
$m_{1/2} = 600$	2.0	−2.8	2.1	−2.7	2.1	−2.5	2.2	−2.2

Table V. $S_{\phi K_S}$ (left) and $\mathrm{Br}[B^- \to \phi K^-] \times 10^6$ (right) at $\tan\beta = 40$ with non-zero ΔA^D_{23} and ΔA^D_{32}.

$\lvert A_0\rvert$	800		600		400		0	
$m_{1/2} = 300$	-0.40	10.0	-0.38	10.0	-0.33	10.1	-0.05	10.0
$m_{1/2} = 400$	-0.11	8.0	-0.05	8.0	0.04	7.9	0.28	8.0
$m_{1/2} = 500$	0.07	6.0	0.16	6.1	0.24	6.1	0.37	6.2
$m_{1/2} = 600$	0.37	6.2	0.44	6.2	0.49	6.2	0.58	6.2

Table VI. $\mathcal{A}_{b\to s+\gamma} \times 10^2$ (left) and $\mathcal{A}_{\phi K^\mp} \times 10^2$ (right) at $\tan\beta = 40$ with non-zero A^D_{23} and A^D_{32}.

$\lvert A_0\rvert$	800		600		400		0	
$m_{1/2} = 300$	-6.3	-3.5	-5.6	-3.4	-5.2	-3.3	-3.6	-2.6
$m_{1/2} = 400$	-3.0	-3.0	-2.1	-2.9	-1.7	-2.6	-0.7	-1.8
$m_{1/2} = 500$	-0.5	-2.9	-0.4	-2.5	-0.2	-2.2	0.2	-1.7
$m_{1/2} = 600$	0.2	-1.7	0.3	-1.4	0.4	-1.2	0.6	-0.8

In Table V and Table VI, we give our results for $\tan\beta = 40$ with non-zero $\Delta A^D_{23(32)}$. The phases ϕ^D_{23} and ϕ^D_{32} are $-(70 \sim 0)^\circ$ and $(80 \sim 110)^\circ$, respectively. $\phi_1 \sim (25 \sim 60)^\circ$, $\phi_3 \sim 25^\circ$ and $\phi_\mu \sim -8^\circ$. The off-diagonal elements $|\Delta A^D_{23(32)}|$ vary from 90 GeV to 250 GeV as $m_{1/2}$ increases. We compare Table V with the results for $\tan\beta = 10$ shown in Table III and we see that only low $m_{1/2}$ can satisfy experimental data for $\tan\beta = 40$. The most important reason for this is that left-right mixing of the second and the third generation decreases significantly with increasing $\tan\beta$. This comes about as follows. The RGE running of $A^D_{23(32)}$ is not sensitive to $\tan\beta$. Therefore, for the same size of $A^D_{23(32)}$ input at the GUT scale, the weak scale values

of $A^D_{23(32)}$ do not differ much for different $\tan\beta$. However, the A^D term enters into the down squark matrix after electroweak symmetry breaking when H_1 (see Eq.(4.20)) grows a vacuum expectation value proportional to $\cos\beta$. Hence the left-right mixing between the second and the third generation in the down squark matrix will be smaller for large $\tan\beta$. For low $m_{1/2}$ this reduction can be compensated by increasing the magnitude of $A^D_{23(32)}$. For example, for $m_{1/2} = 300$ GeV, we use $|A^D_{23(32)}| \sim 90$ GeV in this case compared to 50 GeV in the case of $\tan\beta = 10$ (see Table III). The chargino diagram contribution increases with $\tan\beta$ and can help to generate a large BR. But for large $m_{1/2}$, when the chargino contribution goes down, $|A^D_{23(32)}|$ must become much larger. However, as $|A^D_{23(32)}|$ increases, the pseudoscalar Higgs mass becomes small at the same time (but μ does not get smaller), which prevents $|A^D_{23(32)}|$ from having an unlimited increase. For example, for $m_{1/2} = 600$ GeV and $A_0 = 800$ GeV, $|A^D_{23(32)}| = 250$ GeV generates $m_A = 580$ GeV which is still allowed for the dark matter constraint to be satisfied in the $\tilde{\tau} \leftrightarrow \tilde{\chi}^0$ co-annihilation channel. If $|A^D_{23(32)}|$ is increased more, the pseudoscalar mass gets smaller and the dark matter constraint can still be satisfied due to the available $\chi^0_1\chi^0_1 \to A \to f\bar{f}$ channel. But with a further reduction of the pseudoscalar mass by increasing $|A^D_{23(32)}|$ further, this channel goes away when $m_A < 2m_{\tilde{\chi}^0}$ and we must again satisfy the relic density using the stau-neutralino co-annihilation channel. However, the improvement of $S_{\phi K_s}$ in this scenario is small. For example, for the point mentioned above, $|A^D_{23(32)}|$ can be increased to around 480 GeV with relic density in the $\tilde{\tau} \leftrightarrow \tilde{\chi}^0$ channel but $S_{\phi K_S}$ can only be reduced from 0.37 (see Table V) to 0.22 with the same branching ratio. Thus, the $S_{\phi K_S}$ and the branching ratio still cannot be satisfied.

If we use $\phi^D_{23} = \phi^D_{32}$ (equal phases) we have one less parameter, but that choice will not be able to satisfy experimental results. The reason is that the weak phase from the gluino contributions in the Wilson coefficients C_{8g} and the weak phase from

$\tilde{C}_{8g}$ will cancel when $\phi^D_{23} = \phi^D_{32}$ because C_{8g} depends on A^D_{23} but $\tilde{C}_{8g}$ depends on $(A^D_{32})^\star$. For example, for $\tan\beta = 10$ we find that $S_{\phi K_S} \sim 0.7$ since the gluino contribution dominates at lower $\tan\beta$. At $\tan\beta = 40$, $S_{\phi K_S}$ can reach 0.45 since the chargino contribution is larger at higher $\tan\beta$, but this is not enough to satisfy the data.

5.2. Case II: $|\Delta A^U_{23}| = |\Delta A^U_{32}|$ *and* $\phi^U_{23} = \phi^U_{32}$

In this section we discuss the case $\Delta A^D_{23(32)} = 0$ but $\Delta A^U_{23(32)} \neq 0$. The phases used are similar to those used in first two cases except $\phi^U_{23} = \phi^U_{32}$. This case is more complicated than the $A^D_{23(32)} \neq 0$ case. We find that it is easier to start by comparing them.

The first important change is that the ΔA^U_{32} contribution is much smaller than the ΔA^D_{32} contribution to the mixing between the second and the third generation in the down squark mass matrix due to the suppression by the second generation Yukawa coupling in the RGE of A^D_{32}. (Thus our choice of $\phi^U_{23} = \phi^U_{32}$ has no loss of generality.) Consequently, the size of the Wilson coefficient $\tilde{C}_{8g}$ is significantly reduced. Although ΔA^U_{23} still contributes, that contribution is also reduced (compared to ΔA^D_{23}) due to the RGE. Therefore, compared with the first case the total SUSY contributions are reduced especially for $\tan\beta = 10$ and thus it becomes harder to fit the experimental results, as shown in Table VII.

Another important change is the roles of some experimental constraints which are not important in the first case in the sense that they do not prevent the SUSY contributions from increasing, or at least their limits are not reached when we have solutions satisfying the B-decay data. Below are some comments concerning this:

1. For $\tan\beta = 40$ and low $m_{1/2}$, i.e. 300 GeV, the $\mathrm{Br}[B \to X_s\gamma]$ will constrain the size of $\Delta A^U_{23(32)}$. This is why the $S_{\phi K_S}$ and the branching ratio fit is not as good as the corresponding one shown in Table III for the $A^D_{23(32)} \neq 0$ case.

Table VII. $S_{\phi K_S}$ (left) and $\mathrm{Br}[B^- \to \phi K^-] \times 10^6$ (right) at $\tan\beta = 40$ with non-zero ΔA^U_{23} and ΔA^U_{32}.

$\lvert A_0\rvert$	800		600		400		0		$\lvert\Delta A^U_{23(32)}\rvert$ (GeV)
$m_{1/2} = 300$	0.03	8.4	0.04	9.0	0.01	8.0	0.17	8.0	~ 300
$m_{1/2} = 400$	-0.07	8.5	-0.03	8.4	0	7.1	0.32	6.3	~ 600
$m_{1/2} = 500$	0	6.5	0.07	6.4	0.18	6.0	0.44	6.1	~ 800
$m_{1/2} = 600$	0.27	6.1	0.30	6.1	0.35	6.1	0.51	5.9	~ 1000

Table VIII. $S_{\phi K_S}$ (left) and $\mathrm{Br}[B^- \to \phi K^-] \times 10^6$ (right) at $\tan\beta = 10$ with non-zero ΔA^U_{23} and ΔA^U_{32}.

$\lvert A_0\rvert$	800		600		400		0		$\lvert\Delta A^U_{23(32)}\rvert$ (GeV)
$m_{1/2} = 300$	0.17	6.5	0.16	6.3	0.32	6.1	0.60	5.2	~ 300
$m_{1/2} = 400$	0.37	4.7	0.39	4.6	0.46	4.3	0.62	4.3	~ 550

2. When $m_{1/2}$ increases, the size of $\Delta A^U_{23(32)}$ also needs to be increased. But three other additional constraints are present, i.e ΔM_K and ϵ_K from the $K^0 - \overline{K^0}$ mixing and the mass of smallest up squarks (right-handed stop) $m_{\tilde{t}_R}$. For example, for $m_{1/2} = 500$ and $A_0 = 600$ (and $m_0 = 431$ GeV by the relic density constraint) we get $m_{\tilde{g}} \sim m_{\tilde{q}} \sim 1000$ GeV (where $m_{\tilde{q}}$ is the average squark mass and $m_{\tilde{g}}$ is the mass of the gluino, see [97] for more details) and we find that $\sqrt{|\mathrm{Re}(\delta^d_{12})^2_{LL}|} = 7.1 \times 10^{-2}$ and $\sqrt{|\mathrm{Im}(\delta^d_{12})^2_{LL}|} = 9.7 \times 10^{-3}$ which are allowed by the experimental bounds on ΔM_K and ϵ_K [97] (the sizes of $(\delta^d_{12})_{LR}$, $(\delta^d_{12})_{RL}$ and $(\delta^d_{12})_{RR}$ are around $10^{-8} \sim 10^{-7}$ and thus these bounds can be safely ignored in our case).

3. The situation for the right-handed stop mass is similar to the pseudoscalar Higgs case we mentioned at the end of Case I. We use the $\tilde{\tau} \leftrightarrow \tilde{\chi}^0$ channel to satisfy the dark

matter constraints. Although it's possible to use a larger $A^U_{23(32)}$ which consequently reduces $m_{\tilde{t}_R}$ more and then opens the $\tilde{t}_R \leftrightarrow \tilde{\chi}^0$ channel, the room is small due to the smallness of $m_{\tilde{\chi}^0}$. In addition, the M_K and the ϵ_K bounds become harder to satisfy when $m_{\tilde{t}_R}$ is small. Therefore, as in the case where the pseudoscalar Higgs mass becomes small, possible improvements can not satisfy the experimental results of both $S_{\phi K_S}$ and $\mathrm{Br}[B^- \to \phi K^-]$.

A further difference is the $\tan\beta$ dependence. In Case I, as was discussed above, gluino contributions depend inversely on $\tan\beta$ due to the way that $A^D_{23(32)}$ enters into the down squark mass matrix. But in this case, the gluino contributions are reduced significantly and the chargino plays a more important role, which will be enhanced by $\tan\beta$. Therefore, in this case, we see that larger $\tan\beta$ can satisfy the experimental results at small $m_{1/2}$, but small $\tan\beta$ cannot and that is why we have only given results in Table VIII for two values of $m_{1/2}$ at $\tan\beta = 10$ since higher $m_{1/2}$ cannot improve the situation.

We also comment concerning A_0 and its phase. So far, we have used the phase π for A_0. We find that using a different phase will not improve the results greatly. In general, the improvement is at a few percent level. (This holds also for case I.) For example, in Case II, for $\tan\beta = 40$, $m_{1/2} = 400$ and $A_0 = 800$, we find that using $\alpha_A \sim -95^\circ$ can improve $S_{\phi K_S}$ from -0.04 to -0.06.

Finally we note that the values of $\mathcal{A}_{b\to s+\gamma}$ and $\mathcal{A}_{\phi K^\mp}$ remain small, i.e. $\mathcal{A}_{b\to s+\gamma}$ and $\mathcal{A}_{\phi K^\mp}$ are $-(3 \sim 0)\%$ and $-(3 \sim 1)\%$ at $\tan\beta = 10$, and $-(5 \sim 0)\%$ and $-(3 \sim 1)\%$ at $\tan\beta = 40$.

6. Summary and discussion

Here we have probed the $B \to \phi K$ decays in SUGRA models with CP violating phases to explain the discrepancy between the experimental measurements and the SM predictions of the CP asymmetry of $B^0 \to \phi K_S$ and the branching ratios of the $B \to \phi K$ decays. We have calculated the CP asymmetries of $B^- \to \phi K^-$ and $B \to X_s\gamma$. In our analysis, we implemented all relevant experimental constraints, e.g. Br$[B \to X_s\gamma]$, relic density, $K^0 - \bar{K^0}$ mixing parameters and electron and neutron EDMs, as mentioned in Chapter II. We used the improved QCD factorization method [80, 81] for the calculation of decay amplitudes.

As shown in Section 3, The SM not only can not explain the CP asymmetry of $B^0 \to \phi K_S$, it also fails to satisfy the Br$[B \to \phi K]$ data barring the region of large weak annihilation where the theory is most suspect. We then studied the mSUGRA model and found that it also has the same problem. Therefore, if the current experimental results continue to hold in the future, it will signal the first significant breakdown of the Standard Model and also of mSUGRA. This conclusion is important in the sense that one needs to construct a more complicated SUGRA model to satisfy experimental data which will provide important guidance to our future research on SUSY models and their signals at the accelerator experiments.

In Section 5, we considered the extension of the mSUGRA model by adding non-universal A terms. For a GUT theory, the only natural choice is to have a left-right mixing between the second and the third generation in the up or down quark sectors i.e. $\Delta A_{23}^{U,D}$ and $\Delta A_{32}^{U,D}$ terms. We have examined thoroughly several different possibilities in this extension and their theoretical predictions and have found a large region of parameter space where all experimental results can be satisfied, including the CP asymmetries and branching ratios of the $B \to \phi K$ decays. This result is

obtained without resorting to large weak annihilation amplitudes and so is based on reliable calculations of hadronic decays, and thus provides useful hints for the study of hadronic B decays. Further the size of $\Delta A_{23}^{U,D}$ needed is the same as the other soft breaking terms, and so is not anomalously small or large. Indeed, there are regions in parameter space where the data can be accommodated with $\Delta A_{23}^{D} \approx (20 - 30\%) A_0$, i.e. with only a small perturbation on mSUGRA. Thus, this study also can provide important phenomenological information not only for accelerator physics but also for building models at the GUT scale and for exploring physics beyond it. In this connection, models based on Horava-Witten M-theory can naturally give rise to non-zero values of ΔA_{23}. In [98] it was shown that it was possible to construct a three generation model with $SU(5)$ symmetry using a non-standard embedding based on a torus fibered Calabi-Yau three fold with a del Pezzo base dP_7. The model allowed Wilson line breaking to the Standard Model at M_G, and also had vanishing instanton charges on the physical orbifold plane. If in addition one assumed that the 5-branes in the bulk clustered around the distant plane, one could explain without undue fine tuning the general structure of the quark and lepton mass hierarchies and obtain the LMA solution for neutrino oscillations [98, 99], which will be discussed in detail in the next chapter.

CHAPTER V

YUKAWA TEXTURES, NEUTRINOS AND H-W M-THEORY*

As shown in Chapter I, while the Standard Model (SM) has been successful in fitting all current accelerator data, the origin of the quark and lepton mass spectrum remains a puzzle requiring further understanding. Thus the explanation of the striking hierarchy of masses (e. g. the up to top quark mass ratio is $m_u/m_t \simeq 10^{-5}$) and the hierarchy of elements in the CKM matrix all are beyond the scope of the Standard Model. The matter has been further exacerbated by the discovery of neutrino masses, since now in addition there is need for an explanation of the MNS matrix as well as the origin of the very tiny neutrino masses. A large number of suggestions exist in the literature attempting to explain these properties of quarks and leptons. One approach, starting perhaps with the work of Georgi and Jarlskog [100], suggests that the fundamental origin of quark and lepton masses is to be found at high energies, i. e. the GUT scale, $M_G \cong 3 \times 10^{16}$ GeV, and the complexity we see at low energies arises from the running of the renormalization group equations (RGEs) down to the electroweak scale. This approach, however, has not appeared to be too promising. For example, the u and d Yukawa matrices with five zeros at the GUT scale given in [101] can be written as

$$Y_U = \begin{pmatrix} 0 & \sqrt{2}\lambda^6 & 0 \\ \sqrt{2}\lambda^6 & \sqrt{3}\lambda^4 & \lambda^2 \\ 0 & \lambda^2 & 1 \end{pmatrix} ; \; Y_D = \begin{pmatrix} 0 & 2\lambda^4 & 0 \\ 2\lambda^4 & 2\lambda^3 & 0 \\ 0 & 0 & 1 \end{pmatrix} \tag{5.1}$$

*Tables presented in this chapter are reprinted with permission from "Yukawa Textures, Neutrino Masses and Horava-Witten M-Theory" by R. Arnowitt, B. Dutta, B. Hu, 2004, Nucl. Phys. B 682, 347-366. Copyright 2004 by Elsevier.

where $\lambda = 0.2$ is the Wolfenstein parameter, and the choice of (5.1), when evaluated at the electroweak scale does indeed agree approximately with the quark masses and CKM matrix. However, to generate the experimental hierarchy one has to have entries at the GUT scale of size $\lambda^6 \simeq 10^{-5}$, showing that the problem at the GUT scale is very much the same as at the electroweak scale.

String theory represents at present the only model that has been proposed which in principle can calculate the Yukawa matrices from first principles. Unfortunately, mathematical tools to explicitly do this have not yet been developed. In spite of this, the general formulation of the Yukawa problem in string theory opens new windows for seeing how the quark and lepton hierarchies might naturally have arisen, approaches not available in standard SUGRA GUT theory. In particular, the Horava-Witten heterotic M-Theory [102, 103], which offers a natural explanation of why grand unification can occur at M_G rather than the Planck scale M_P, has had significant development (see [99] and references therein) giving rise to three generation models with the SM low energy gauge group $SU(3) \times SU(2) \times U(1)$. In this model, physical space is one of two 10 dimensional (10D) orbifold planes separated by a finite distance in the 11th dimension, the theory obeying S^1/Z_2 symmetry in the 11th dimension. Six of the 10 dimensions are compactified to a Calabi-Yau (C-Y) threefold, the remaining four being Minkowski space. An array of six dimensional 5-branes perpendicular to the 11th dimension can exist between the two orbifold planes. While it is not possible to make first principle calculations, one can examine whether the general structure of such a theory can replicate the SM at low energy. In this connection, it was seen in [98] that the general structure of the quark mass matrices can arise without undue fine tuning if the 5-branes lie close to the distant orbifold plane, and the instanton number of the physical orbifold plane, $\beta^{(0)}$ vanished. It was explicitly shown in [98] that a three generation model with $\beta^{(0)} = 0$ and SM gauge group indeed can exist for

a torus fibered Calabi-Yau (with two sections) with del Pezzo base dP_7. The quark and CKM matrix were calculated for a model of this type in agreement with data, and it was shown also in approximate analytic calculations how the mass hierarchies can arise without undue fine tuning due to the general structure of the Kahler potential.

Here we extend the analysis of [98] in two directions. We first include the charged lepton mass matrix and obtain the mass hierarchies experimentally seen. We then consider neutrino masses. The conventional way for accounting for the very small mass of neutrinos is the seesaw mechanism [104, 105, 106] which gives rise to Majorana neutrino masses. We consider here, however, a new way of achieving small neutrino masses based on the structure of the Kahler potential. This mechanism is different from the seesaw mechanism, and gives rise to Dirac masses for the neutrinos. Neutrino masses and the MNS matrix [107] are calculated consistent with the large mixing angle (LMA) analysis of the solar, atmospheric, reactor and long baseline neutrino data (e.g. see [108] for a global analysis in the context of three-neutrino oscillations).

In the next section we first give a brief review of M-Theory, and the basic results obtained in [98] for torus fibered Calabi-Yau manifolds. In Section 2 we review and update the results of [98] for the quark masses and extend this analysis to the lepton sector. Then we introduce the new mechanism to obtain small neutrino masses and show an explicit example for the masses and mixing angles for this model. A discussion is given in the last section.

1. Horava-Witten Kahler potential

The Horava-Witten M-Theory is concerned with 11 dimensional supergravity on an orbifold $M_{10} \times S^1/Z_2$, where Z_2 is reflection of the 11th coordinate. One can think of this space as an 11 dimensional space M_{11} bounded by two 10 dimensional orbifold

planes M_{10} at $x^{11} = 0$ and $\pi\rho$. In the simplest case, M_{10} is the product space $M_4 \times X$ where M_4 is Minkowski space and X is a (compact) C-Y threefold, the physical world living on one of the orbifold planes (e.g. $x^{11} = 0$), the other orbifold plane being a "hidden" sector. In addition, there may be six dimensional 5-branes lying along x^{11} at bulk points x_n with $0 < x_n < \pi\rho$, parallel to the orbifold planes, each with four dimensions spanning M_4, the additional two dimensions wrapped around a holomorphic curve in the Calabi-Yau space. The construction of a consistent theory involves a remarkable set of interlocking constraints due to anomaly cancellation, gauge invariance, and local supersymmetry leading naturally to a theory which possesses a number of properties appropriate for phenomenology. Thus there must be E_8 gauge interactions with chiral multiplets on each M_{10} orbifold plane (SO(32) being excluded) which can easily be broken on the physical plane to the SM group by Wilson lines. The 10D gauge coupling constant, λ, is uniquely determined in terms of the 11D Planck mass, $\kappa^{-2/9}$, leading to the result that the fundamental scale of nature, the 11D Planck mass, is $\mathcal{O}(M_G)$, and explaining why grand unification occurs at M_G rather than the 4D Planck mass (which is a derived quantity). Finally, a consistent theory exists only as a quantum theory (the classical theory being inconsistent), something one would hope might be true for any fundamental theory. Much progress has been made in showing what the low energy structure of such a theory might be, and models with three generations of quarks and leptons obeying the SM gauge group have been constructed. While the details of the construction of the theory given in [102, 103] is rather intricate, it is possible to see how the different elements interact to produce a physically interesting model and so we first briefly summarize this construction. We then give the relevant formulae needed to examine the low energy structure. Details of the latter can be found in [109], and for the specific model considered here in [98].

The field content of 11D supergravity is the metric g_{IJ}, the gravitino ψ_{IJ}, the

three form C_{IJK} and its field strength G_{IJKL}. (In lowest order $G_{IJKL} = d_I C_{JKL}$.) The Bose part of the Lagrangian is :

$$\begin{aligned} L_S &= \frac{1}{\kappa^2}\int_{M^{11}} d^{11}x\sqrt{g}\left(-\frac{1}{2}R - \frac{1}{48}G_{IJKL}G^{IJKL}\right. \\ &\quad \left. -\frac{\sqrt{2}}{3456}\epsilon^{I_1 I_2 \ldots I_{11}} C_{I_1 I_2 I_3} G_{I_4 \ldots I_7} G_{I_8 \ldots I_{11}}\right). \end{aligned} \tag{5.2}$$

where the field strengths obey the field equations $D^I G_{IJKL} = 0$, and the Bianchi identity $dG_{IJKLM} = 0$. Here κ is the 11D gravitational constant. The Horava-Witten theory comes about as follows. While in a smooth manifold 11D supergravity has no anomalies, on an orbifold anomalies arise at the fixed points $x = 0$ and $x = \pi\rho$. To cancel these, it is necessary to put Yang Mills multiplets on each M_{10} orbifold plane, and the cancellation occurs only if the gauge group on each manifold is (the phenomenologically desirable) E_8. To lowest order, the Yang Mills Lagrangian on each M_{10} reads then:

$$L_{YM} = -\frac{1}{\lambda^2}\int_{M^{10}} d^{10}x\sqrt{g}\ \mathrm{tr}\left(\frac{1}{4}F_{AB}F^{AB} + \frac{1}{2}\bar{\chi}\Gamma^A D_A \chi\right). \tag{5.3}$$

where $A, B = 1, 2 \ldots 10$, and χ is the associated gaugino. However, (5.3) is not locally supersymmetric, and one must proceed in the usual fashion to add additional interactions and modifications of the transformation laws to achieve local supersymmetry. As usual, this involves coupling the gravitino to the Yang Mills supercurrent. However, unlike the case where the Yang Mills and supergravity multiplets live in the same space, the gravitino here lives in the 11D bulk, while the Yang Mills multiplet is constrained to live in 10D. For this situation, a locally supersymmetric Yang Mills theory cannot be achieved simply by adding interactions on the orbifold plane. It turns out that a supersymmetric theory can be achieved only by modifying the Bianchi identities to read

$$dG_{11\,ABCD} = 8\pi^2\sqrt{2}\frac{\kappa^2}{\lambda^2}\Sigma_0^{N+1} J^{(n)}\delta(x^{11} - x_n). \tag{5.4}$$

where $x_0 = 0$, $x_{N+1} = \pi\rho$ and x_n, $n = 1 \ldots N$ are the positions of the five branes,

$$J^{(0,N+1)} = -\frac{1}{16\pi^2}\left(\operatorname{tr} F \wedge F - \frac{1}{2}\operatorname{tr} R \wedge R\right)_{x^{11}=0,\pi\rho}. \tag{5.5}$$

and $J^{(n)}$, $n = 1 \ldots N$ are sources from the 5-branes. With (5.4), the total supergravity + (modified) Yang Mills Lagrangian can be made locally supersymmetric. However, having gained supersymmetry, one has lost Yang Mills gauge invariance. For while (5.4) implies that G_{ABCD} is gauge invariant, the corresponding potential $C_{11\,AB}$ now is not, i.e. under a Yang Mills gauge transformation one has

$$\delta C_{11\,AB} = -\frac{\kappa^2}{6\sqrt{2}\lambda^2}\left[\operatorname{tr}\left(\epsilon F_{AB}\delta(x^{11})\right) + \operatorname{tr}\left(\epsilon F_{AB}\delta(x^{11} - \pi\rho)\right)\right]. \tag{5.6}$$

which implies the $C \wedge G \wedge G$ term of (5.2) is not gauge invariant. Thus the classical theory is not gauge invariant, and a consistent classical theory does not exist. However, in the quantum theory, there is in addition the 10D Majorana-Weyl anomaly, and due to unique features of the E_8 group can cancel the loss of gauge invariance of the "Green-Schwarz" $C \wedge G \wedge G$ term provided

$$\lambda^2 = 2\pi(4\pi\kappa)^{2/3}. \tag{5.7}$$

Thus only a consistent quantum theory can be built, and this quantum theory determines the 10D gauge coupling constant in terms of the 11D gravitational constant.

(5.7) leads immediately to interesting phenomenological consequences. For compactifying M_{11} on a Calabi-Yau manifold, one has to lowest order for the 4D gauge coupling constant and Newton constant [110]

$$\alpha_G = \frac{(4\pi\kappa^2)^{2/3}}{2\mathcal{V}}; \quad G_N = \frac{\kappa^2}{16\pi^2\mathcal{V}\rho} \tag{5.8}$$

where $\mathcal{V}$ is the Calabi-Yau volume. Setting $\mathcal{V}^{1/6} = 1/M_G$ (so that grand unification occurs at the compactification scale as required by the LEP data) and using $\alpha_G = 1/24$, one finds that the fundamental 11D Planck mass is $\kappa^{-2/9} \cong 2M_G$ and $\pi\rho^{-1} \cong$

4.7×10^{15} GeV. Alternately one may say that the 11D Planck mass is the fundamental scale and it sets the GUT scale, while the largeness of the 4D Planck mass is due mostly to accidental 4π factors arising in the analysis.

We now summarize the basic formulae of [109] and [98] needed to build a phenomenologically acceptable theory. The sources $J^{(n)}$ of (5.4) play an important role in building a model. Thus if integrated over a set of independent 4 cycles C_{4i}, they define integer charges:

$$\beta_i^{(n)} = \int_{C_{4i}} J^{(n)} \tag{5.9}$$

and (5.4) then implies $\Sigma\beta_i^{(n)} = 0$. Here $\beta_i^{(0)}$ and $\beta_i^{(N+1)}$ are the instanton charges on the orbifold planes and $\beta_i^{(n)}$ $(n = 1\ldots N)$ are the magnetic charges of the 5-branes. The existence of non-zero instanton Yang Mills fields with gauge group G on the orbifold plane implies that E_8 breaks into $G \times H$ where H is the remaining symmetry at the GUT scale of the physical theory. We chose here $G = SU(5)$ so that $H = SU(5)$.

Chiral matter arises from the components of the Yang Mills multiplet in the Calabi-Yau part of the M_{10} orbifold [109]. Thus labeling the C-Y indices by holomorphic (anti-holomorphic) coordinates $a(\bar{a}) = 1, 2, 3$, then one can expand e.g. $F_{\mu\bar{b}}$ in terms of a basis set of functions u_I^x in the C-Y space (I is a family index and x a representation index), the coefficients in the Minkowski space being the scalar components of the chiral multiplets $C(R)^{Ip}$ (where R is the representation):

$$F_{\mu\bar{b}} = \sqrt{2\pi\alpha_G}\sum_R u^x_{I\bar{b}}(R)\, T_{xp}(R)(D_\mu C(R))^{Ip}. \tag{5.10}$$

In terms of these quantities, one then defines the metric

$$G_{IJ}(a^i; R) = \frac{1}{vV}\int_X \sqrt{g} g^{a\bar{b}} u_{Iax}(R) u^x_{J\bar{b}}(R) \tag{5.11}$$

and the Yukawa couplings [109]

$$\lambda_{IJK}(R_1,R_2,R_3)=\int_X \Omega\wedge u_I^x(R_1)\wedge u_J^y(R_2)\wedge u_K^z(R_3) f_{x,y,z}^{(R_1,R_2,R_3)} \tag{5.12}$$

where Ω is the covariantly constant (3,0) form, f projects out the gauge singlet parts, and $\mathcal{V}\equiv vV$ is the volume of the Calabi-Yau space while v is the coordinate volume:

$$V=\frac{1}{v}\int_X d^6x\sqrt{g};\;\; v=\int_X d^6x \tag{5.13}$$

In addition one defines the S, T^i and 5-brane moduli by

$$Re(S)=V;\;\; ReT^i=V^{-1/3}Ra^i;\;\; ReZ_n=z_n \tag{5.14}$$

where the modulus R is the orbifold radius divided by ρ and $z_n=x_n/\pi\rho$. V can be expressed in terms of the a^i moduli by $V(a)=\frac{1}{6}d_{ijk}a^ia^ja^k$ where d_{ijk} are the Calabi-Yau intersection numbers :

$$d_{ijk}=\int_X \omega_i\wedge\omega_j\wedge\omega_k \tag{5.15}$$

Following the techniques of [110], the field equations and Bianchi identities in (5.4) were solved in the presence of 5-branes to leading order $O(\kappa^{2/3})$ [109] leading to an effective four dimensional Lagrangian at compactification scale M_G. We now state the results that were obtained. The gauge kinetic functions on the orbifold planes are given by

$$\begin{aligned} f^{(1)} &= S+\epsilon T^i\left(\beta_i^{(0)}+\sum_{n=1}^{N}(1-Z_n)^2\beta_i^{(n)}\right)\\ f^{(2)} &= S+\epsilon T^i\left(\beta_i^{(N+1)}+\sum_{n=1}^{N}Z_n^2\beta_i^{(n)}\right) \end{aligned} \tag{5.16}$$

where

$$\epsilon=\left(\frac{\kappa}{4\pi}\right)^{2/3}\frac{2\pi^2\rho}{\mathcal{V}^{2/3}} \tag{5.17}$$

The matter Kahler potential, $K = Z_{IJ}\bar{C}^I C^J$, on the physical orbifold plane at $x^{11} = 0$ has the Kahler metric

$$Z_{IJ} = e^{-K_T/3}\left[G_{IJ} - \frac{\epsilon}{2V}\tilde{\Gamma}^i_{IJ}\sum_{n=0}^{N+1}(1-z_n)^2\beta_i^{(n)}\right] \tag{5.18}$$

where

$$K_T = -\ln[\frac{1}{6}d_{ijk}(T^i+\bar{T^i})(T^j+\bar{T^j})(T^k+\bar{T^k})] \tag{5.19}$$

$$\tilde{\Gamma}^i_{IJ} = \Gamma^i_{IJ} - (T^i+\bar{T^i})G_{IJ} - \frac{2}{3}(T^i+\bar{T^i})(T^k+\bar{T^k})K_{Tkj}\Gamma^j_{IJ} \tag{5.20}$$

and

$$K_{Tij} = \frac{\partial^2 K_T}{\partial T_i \partial \bar{T^j}};\ \Gamma^i_{IJ} = K_T^{ij}\frac{\partial G_{IJ}}{\partial T^j} \tag{5.21}$$

The Yukawa matrices are

$$Y_{IJK} = 2\sqrt{2\pi\alpha_G}\lambda_{IJK} \simeq 1.02\lambda_{IJK} \tag{5.22}$$

for $\alpha_G = 1/24$. The Kahler metric on the distant orbifold plane at $x^{11} = \pi\rho$ is given by (5.18) with $z_n \to (1-z_n)$.

2. Yukawa textures

The Yukawa couplings are given in (5.12) and (5.22) as integrals over the C-Y space. A priori there is no reason to suggest that a hierarchy such as (5.2) should arise and one expects that the non-zero entries to be $O(1)$. Similarly, one expects a priori that the non-zero elements of G_{IJ} in (5.11) be of $O(1)$. However, a mild hierarchy can develop in the Kahler metric of (5.18) if the 5-branes all lie close to the distant orbifold plane, i. e. $d_n = 1 - z_n \cong 0.1$, and provided also $\beta^{(0)} = 0$. Then the second term will be small compared to the first ($\epsilon \cong 0.9$), and the model of [98] assumed that G_{IJ} contributes only to the first two generations of the u quark and d_L

quark (which appear together in the $SU(5)$ 10 representation) but to all generations of d_R, while the second term contributes to all generations but is then dominant for the third generation of u_L, u_R, d_L. (That a C-Y manifold exits with $\beta^{(0)} = 0$ with three generations and a SM gauge group is non-trivial and was explicitly shown to be possible in [98].) When the Kahler metric was diagonalized to a unit matrix, it was seen that this idea was sufficient to generate a satisfactory explanation of the more extreme Yukawa hierarchies at the electroweak scale, and we extend this idea here to the lepton sector. Thus the Kahler metric has the general form

$$Z^F = f_T \begin{pmatrix} 1 & O(1) & O(d^2) \\ O(1) & O(1) & O(d^2) \\ O(d^2) & O(d^2) & O(d^2) \end{pmatrix} \tag{5.23}$$

where F stands for the different matter fields: $q = u_L, u_R, d_L$, $l = (\nu_L, e_L)$ and $e = e_R$ and f_T is given from Eq.(5.18) to be $e^{-K_T/3}$. We assume that G_{IJ} has non-zero elements of $O(1)$ for all generations of d_R. (For convenience, we've re-scaled the Z^F_{11} entry in (5.23) to 1.) The hierarchy then arises when one transforms the Z_{IJ} to the unit matrix by a unitary matrix U and a diagonal scaling matrix S to obtain the canonical matter fields $C_F^{I\,\prime}$:

$$C_F^I = \frac{1}{\sqrt{f_T}} (U^{(F)} S^{(F)})_{IJ} C_F^{J\prime} \tag{5.24}$$

where

$$\mathrm{diag} S^{(F)} = (\lambda_{F1}^{-1/2},\, \lambda_{F2}^{-1/2},\, \lambda_{F3}^{-1/2}). \tag{5.25}$$

and λ_{Fi}, $i = 1, 2, 3$ are the eigenvalues of Z^F_{IJ}/f_T. A similar transformation is made on the Higgs fields contribution to the Kahler potential

$$f_T G_{H_{1,2}} \bar{H}_{1,2} H_{1,2} \tag{5.26}$$

with rescaling of $H_{1,2}$:

$$H_{1,2} = \frac{1}{\sqrt{f_T G_{H_{1,2}}}} H'_{1,2} \tag{5.27}$$

Before making the transformation of (5.24), The Yukawa contribution to the superpotential is [109]

$$W_Y = e^{\frac{1}{2}K_m}\frac{1}{3}Y_{IJK}C^I C^J C^K \tag{5.28}$$

where $K_m = \ln(S+\bar{S}) + K_T$ is the moduli contribution to the Kahler potential. From (5.14) and (5.19), one has

$$K_m = -ln(2V) - ln(8R^3). \tag{5.29}$$

Written in terms of SM fields W_Y then is

$$W_Y = \frac{1}{4R^{3/2}V^{1/2}}(Y^{(u)}q_L H_2 u_R + Y^{(d)}q_L H_1 d_R + Y^{(e)}l_L H_1 e_R). \tag{5.30}$$

and after the transformation to the canonical matter fields one has

$$W_Y = u'_L\lambda^{(u)}u'_R H'_2 + d'_L\lambda^{(d)}d'_R H'_1 + e'_L\lambda^{(e)}e'_R H'_1. \tag{5.31}$$

where $\lambda^{(u,d,e)}$ are give by

$$\lambda^{(u)}_{IJ} = \frac{1}{8\sqrt{2}}\frac{1}{R^3V^{1/2}}\frac{1}{\sqrt{G_{H_2}}}(S^{(q)}\tilde{U}^{(q)}Y^{(u)}U^{(u)}S^{(u)})_{IJ} \tag{5.32}$$

$$\lambda^{(d)}_{IJ} = \frac{1}{8\sqrt{2}}\frac{1}{R^3V^{1/2}}\frac{1}{\sqrt{G_{H_1}}}(S^{(q)}\tilde{U}^{(q)}Y^{(d)}U^{(d)}S^{(d)})_{IJ} \tag{5.33}$$

$$\lambda^{(e)}_{IJ} = \frac{1}{8\sqrt{2}}\frac{1}{R^3V^{1/2}}\frac{1}{\sqrt{G_{H_1}}}(S^{(l)}\tilde{U}^{(l)}Y^{(e)}U^{(e)}S^{(e)})_{IJ} \tag{5.34}$$

We use here the notation "$\sim$" for transpose. In (5.31), $\lambda^{(u,d,e)}$ play the role of the Yukawa matrices at the GUT scale in the phenomenological analyses such as in [101]. However, in general they are not symmetric matrices and so M-Theory textures are uniquely different from what has previously been considered in phenomenological analyses. In brief, it is the smallness of the third generation eigenvalues of the Kahler matrices appearing in the denominators of (5.32-5.34) (from the factor S of (5.25)) that give rise to the large third generation masses.

In [98] we saw for the case of $\tan\beta = 3$ how the above Yukawa matrices gave rise to the experimental quark masses and CKM matrix elements at the electroweak scale, and we showed there analytically how the hierarchies arose naturally without undue fine tuning. We now update this analysis for the case of $\tan\beta = 40$, and extend the discussion to include the lepton sector. A choice of Kahler metric and Yukawa matrices that satisfy all the current experimental data are given by

$$
\begin{aligned}
Z^u &= f_T \begin{pmatrix} 1 & 0.3452 & 0 \\ 0.3452 & 0.1311 & 0.006365 \\ 0 & 0.006365 & 0.00344 \end{pmatrix} , \\
Z^d &= f_T \begin{pmatrix} 1 & 0.496 & 0 \\ 0.496 & 0.564 & 0.435 \\ 0 & 0.435 & 0.729 \end{pmatrix} , \\
Z^l &= f_T \begin{pmatrix} 1 & -0.547 & 0 \\ -0.547 & 0.432 & 0.025 \\ 0 & 0.025 & 0.09 \end{pmatrix} , \\
Z^e &= f_T \begin{pmatrix} 1 & 0.624 & 0 \\ 0.624 & 0.397 & 0.00574 \\ 0 & 0.00574 & 0.004407 \end{pmatrix} , \\
\mathrm{diag}Y^{(u)} &= (0.0114,\, 0.0597,\, 0.104\, \exp[0.65\pi i]) , \\
\mathrm{diag}Y^{(d)} &= (2.052,\, 0.2565,\, 1.8297) , \\
\mathrm{diag}Y^{(e)} &= (0.307,\, 3.789,\, 1.821). \qquad (5.35)
\end{aligned}
$$

The Z^F_{23}, Z^F_{32} and Z^F_{33} entries for $F = u, l, e$ are $O(d^2)$ (for $d = 0.1$) as required by (5.23). For simplicity we have assumed that the q and u quarks have identical Kahler matrices and have the maximum number of zero entries, and that the Yukawa

matrices are diagonal. One phase is assumed in the Yukawa matrices to account for CP violation. To compare with low energy data, we use one loop Yukawa RGEs and two loop gauge RGEs to evaluate the Yukawa couplings at the electroweak scale, which we take to be m_t. Below m_t we assume that the Standard Model holds and include in our calculations the QCD corrections (which are quite significant). The QCD correction factors used were $\eta_c = 2$, $\eta_u = 2.5 = \eta_d$, $\eta_b = 1.6$ and $\eta_s = 2.5$. Diagonalization of the low energy Yukawa matrices then allows one to generate the low energy quark and lepton masses and the CKM matrix elements. The results are shown in Table IX (where experimental values for lepton and quark masses are from [1] and CKM entries from [111] unless otherwise noted), and are in good agreement with experiment. Of course in a fundamental analysis, the precise entries in (5.35) arise from integrals over the Calabi-Yau space, an analysis that cannot at this stage be performed. However, our discussion has shown that the general structure of the Kahler metric and Yukawa couplings arising in our Horava-Witten model can lead to low energy quark and lepton spectra consistent with all current experiments without the fine tuning used in phenomenological analyses.

Without knowledge of the value of the factors $R^3 V^{1/2} \sqrt{G_{H_{1,2}}}$ in the denominators of (5.32-5.34), Kahler textures can only determine the mass ratios. As in [98], we use the top Yukawa at the GUT scale to determine the value of this common factor. If we write $V = r^6$, where r is the mean radius of the Calabi-Yau manifold divided by the co-ordinate radius, then for $G_{H_{1,2}} = 1$, one finds that

$$R \times r = 6.82. \tag{5.36}$$

In the next section, we will show that R and r can be determined separately if massive neutrinos enter our model via the mechanism proposed there.

Table IX. Quarks and leptons masses and CKM matrix elements obtained from the model with parameters given in (5.35). Masses are in GeV.

Quantity	Theoretical Value	Experimental Value
m_t(pole)	175.2	174.3 ± 5.1
$m_c(m_c)$	1.27	1.0-1.4
m_u(1 GeV)	0.00326	0.002-0.006
$m_b(m_b)$	4.21	4.0-4.5
m_s(1 GeV)	0.086	0.108-0.209
m_d(1 GeV)	0.00627	0.006-0.012
m_τ	1.78	1.777
m_μ	0.1054	0.1056
m_e	0.000512	0.000511
$\|V_{us}\|$	0.221	0.2210 ± 0.0023
$\|V_{cb}\|$	0.042	0.0415±0.0011
$\|V_{ub}\|$	4.96×10^{-3}	$3.80^{+0.24}_{-0.13} \pm 0.45 \times 10^{-3}$
$\|V_{td}\|$	6×10^{-3}	$9.2 \pm 1.4 \pm 0.5 \times 10^{-3}$
$\sin 2\beta$	0.803	0.731 ± 0.056 [76]

3. Neutrino masses and oscillations

In the last section we presented a way to generate the Yukawa textures in the quark and lepton sectors whose structures are the same as the SM. The consequence of the masslessness of neutrinos in the SM is that the mass eigenstates of leptons are identical to their gauge or flavor eigenstates and, unlike the quark sector which has a CKM mixing matrix, the lepton sector does not. Therefore, there is no oscillations between neutrinos in the SM. However, the neutrino experiments of Super-Kamiokande [112,

113], SNO [114, 115] and KamLAND [116] have shown the existence of neutrino oscillations which indicates that neutrinos are actually massive particles. In this section we will show that massive neutrinos can be included in our model and their masses and mixings can be fitted into the large mixing angle (LMA) solution [117].

The simplest way to include massive neutrinos to our model is to associate a right-handed neutrino to every left-handed neutrino and insert by hand a term proportional to

$$Y^{(\nu)} l_L H_2 \nu_R \tag{5.37}$$

into superpotential (5.30). However, the Yukawa couplings in the neutrino sector have to be extremely small and thus this solution is theoretically less interesting unless there is a mechanism behind it. The most widely used way to overcome this problem is the seesaw mechanism [104, 105, 106]. In seesaw models, besides the usual Dirac mass terms (which are approximately the same size as other fermion masses), one introduces additional very large Majorana masses which enter in the off-diagonal entries of the neutrino mass matrix. As a consequence, some eigenvalues are suppressed to the desired values when the diagonalization of neutrino mass matrix takes place. The physical neutrinos in seesaw models are then of Majorana type while other leptons and quarks are Dirac fermions. Here we propose a new way to generate neutrino masses. In our model, neutrinos are of Dirac type and thus the similarity between leptons and quarks is preserved and no neutrinoless double beta decay exists. We will see that our new mechanism provides a reasonable physical explanation to the origin of term (5.37).

The Kahler potential in principle can have gravitationally coupled trilinear terms which are usually ignored as they generally are of negligible size. However, we assume here that our Kahler potential at the GUT scale contains the holomorphic cubic term

$K^{(3)} = K_\nu + K_\nu{}^\dagger$ where

$$K_\nu = \kappa_{11} Y^{(\nu)} l_L H_2 \nu_R \tag{5.38}$$

where $1/\kappa_{11}$ is the 11 dimensional Planck mass (i.e. $1/\kappa_{11} \simeq M_G$) and Y^ν is a Yukawa matrix. We note that (5.38) is the only gauge invariant holomorphic cubic lepton term involving ν_R and that κ_{11} is the natural scale for Horava-Witten theory. The Yukawa contribution to the superpotential is still given by (5.31). One can transfer K_ν from the Kahler potential to the superpotential by a Kahler transformation ($1/\kappa_4$ is the 4D Planck mass):

$$\begin{aligned} K &\rightarrow K - K^{(3)}, \\ W &\rightarrow e^{\kappa_4{}^2 K_\nu} W = W + \kappa_4{}^2 K_\nu W + \cdots \end{aligned} \tag{5.39}$$

Now when supersymmetry breaks, the superpotential W will grow a VEV of size:

$$\langle W \rangle \cong \frac{1}{\kappa_4{}^2} M_S \tag{5.40}$$

where M_S is of electroweak size. Consequently, after supersymmetry breaking, an additional term appears in superpotential (5.31):

$$\frac{M_S}{M_G} Y^{(\nu)} l_L H_2 \nu_R. \tag{5.41}$$

We can now proceed as in the last Section. First diagonalize and rescale the Kahler matrices Z_{IJ} of ν_R and other fields to the unit matrix. Then make the necessary transformations in the superpotential to the canonical normalized fields. The term giving rise to neutrino masses can then be written as

$$\nu'_L \lambda^{(\nu)} \nu'_R H'_2 \tag{5.42}$$

where

$$\lambda^{(\nu)}_{IJ} = \frac{1}{\sqrt{2}} \frac{1}{R^{3/2}} \frac{1}{\sqrt{G_{H_2}}} \frac{M_S}{M_G} (S^{(l)} \tilde{U}^{(l)} Y^{(\nu)} U^{(\nu)} S^{(\nu)})_{IJ} \tag{5.43}$$

Note that the overall coefficient in (5.43) is different from the one in (5.32-5.34) because the neutrino term originates from the Kahler potential, not the superpotential (5.28) which has the additional coefficient $e^{\frac{1}{2}K_m}$. It is thus possible to use the experimental neutrino mass square differences to determine R. In the example given below, we find that $R = 2.13$ produces acceptable neutrino masses (we assume $M_S = 1$ TeV in our calculation), and from Eq.(5.36), one finds that $r = 3.20$. At the weak scale, after the diagonalization of charged lepton and neutrino Yukawa matrices, the Maki-Nakagawa-Sakata (MNS) lepton mixing matrix arises. We follow the standard parameterization [1] (the phase similar to the one in the CKM matrix is ignored):

$$V_{MNS} = \begin{pmatrix} c_{12}c_{13} & s_{12}c_{13} & s_{13} \\ -s_{12}c_{23} - c_{12}s_{23}s_{13} & c_{12}c_{23} - s_{12}s_{23}s_{13} & s_{23}c_{13} \\ s_{12}s_{23} - c_{12}c_{23}s_{13} & -c_{12}s_{23} - s_{12}c_{23}s_{13} & c_{23}c_{13} \end{pmatrix}. \tag{5.44}$$

where $c_{ij} = \cos\theta_{ij}$, $s_{ij} = \sin\theta_{ij}$ and $i, j = 1, 2, 3$.

The following is an example at $\tan\beta = 40$. We use the lepton entries of (5.35), and the following neutrino Kahler and Yukawa matrices at M_G:

$$Z^{\nu} = f_T \begin{pmatrix} 1 & -0.465 & 0 \\ -0.465 & 0.3105 & 0.0254 \\ 0 & 0.0254 & 0.027 \end{pmatrix}; \tag{5.45}$$

$$\text{diag}Y^{(\nu)} \;=\; (4,\, 0.4,\, 4). \tag{5.46}$$

The neutrino mass square differences and mixing angles at the weak scale are then calculated to be:

$$\Delta m^2_{21} \;=\; 5.5 \times 10^{(-5)}\ \text{eV}^2; \tag{5.47}$$

$$\Delta m^2_{32} \;=\; 2.7 \times 10^{(-3)}\ \text{eV}^2; \tag{5.48}$$

$$\tan^2\theta_{12} = 0.42; \quad \tan^2\theta_{23} = 0.93. \tag{5.49}$$

with $|U_{e3}| = 0.005$. Since our model is a complete model of neutrino masses, we can calculate all the masses themselves and not just the mass square differences. For the above example we find

$$m_1 = 6.5 \times 10^{-4}\ \text{eV};\quad m_2 = 7.4 \times 10^{-3}\ \text{eV};\quad m_3 = 5.2 \times 10^{-2}\ \text{eV} \tag{5.50}$$

consistent with cosmological constraints on neutrino masses [118].

The analysis of solar and KamLAND data in terms of two neutrino oscillations gives for the LMA solution [113]:

$$0.20 \leq \tan^2\theta_S \leq 0.68\,; \quad 5.6 \times 10^{-5} \leq \Delta m_S^2/\text{eV}^2 \leq 8.9 \times 10^{-5} \tag{5.51}$$

where Δm_S^2 is the solar neutrino mass square difference and θ_S is the corresponding mixing angle and the ranges in (5.51) (and (5.52) below) are 3σ around the central value. The analysis of Super-Kamiokande and K2K data shows for the LMA solution [119]:

$$0.85 \leq \sin^2 2\theta_A \leq 1\,; \quad 1.4 \times 10^{-3} \leq \Delta m_A^2/\text{eV}^2 \leq 3.8 \times 10^{-3} \tag{5.52}$$

where Δm_A^2 and θ_A are the relevant mass square difference and mixing angle for the atmospheric neutrino oscillation.

Since in our case $|U_{e3}| \cong 0$, solar and atmospheric neutrino oscillations decouple [108, 120]. Therefore the two neutrino oscillation analysis can be applied to our case with the effective mixing angles given by:

$$\theta_S = \theta_{12}\,,\quad \theta_A = \theta_{23}. \tag{5.53}$$

(5.47)-(5.49), (5.51) and (5.52) show that our results agree with the current LMA solution quite well.

4. Summary and discussion

Here we extend a model of the quark mass hierarchy based on the Horava-Witten M-Theory [98] to include charged leptons and massive neutrinos. The model is based on the assumptions that five branes exists in the bulk lying near the distant orbifold plane (i. e. about 90% of the way from the physical plane), and that the instanton charges on the physical plane vanish. This can gave rise to a three generation model with the Standard Model gauge group at the GUT scale. While one cannot calculate Yukawa couplings in M-Theory (they involve integrals over the Calabi-Yau space) these constraints were sufficient to qualitatively account for the quark mass hierarchy at the electroweak scale without undue fine tuning. The mechanism that achieved this was that the five brane contribution to the Kahler potential gave rise to small Kahler matrix eigenvalues, and the quark masses were proportional to the reciprocal square root of the eigenvalues when the kinetic energy was put into canonical form. We saw that the same mechanism also gave rise qualitatively to the hierarchy of charged lepton masses, again without any excessive fine tuning.

Neutrino masses can arise in these models if a right handed neutrino exists in the massless particle spectrum. Then one can assume that the Kahler potential has a cubic holomorphic contribution of the form of (5.38), the interaction being scaled by the 11 dimensional Planck mass (the basic parameter of Horava-Witten theory). When transformed to the superpotential by a Kahler transformation, this term gives rise to neutrino masses of the correct size after supersymmetry breaking. (Thus the mechanism being used here for the neutrino masses is similar to the one previously used to generate a μ parameter of electroweak size [121].) it is possible then to chose natural sized values for the Yukawa and Kahler matrix entries to generate masses and CKM and MNS mixing angles in agreement with all low energy data. The neutrinos

in this model are Dirac, and so will exclude neutrinoless double beta decay.

Aside from the Kahler and Yukawa matrices, the quark, lepton and neutrino properties depend on the Calabi-Yau volume modulus $\mathcal{V}$ which we have parameterized by $V^{1/6} = r$ and the radius modulus R. We have found that all the quark, lepton and neutrino masses can be fit satisfactorily with r and R of $O(1)$. Thus for the example in text for $\tan\beta = 40$ we found $R = 2.13$ and $r = 3.20$. One important feature of this Horava-Witten model that has not been addressed here is how to stabilize the position of the 5-brane close to the distant orbifold plane. One possibility may involve quantum corrections, e.g. membrane potentials between the 5-brane and the orbifold planes [122, 123, 124, 125].

CHAPTER VI

CONCLUSION

Here we have discussed some important topics in SUSY phenomenology, including the muon magnetic moment, $B \to \phi K$ decays and the phenomenological aspects of a Horava-Witten M-Theory model. Our studies are carried out in the framework of the SUGRA models. We considered all relevant experimental bounds in our analyses.

In the study of the muon magnetic moment we found that the current $g_\mu - 2$ data can impose a strong constraint on the SUSY parameter space and hence can provide important information for the dark matter detection experiments and accelerator experiments. As explained in Chapter 2, a large muon magnetic moment can potentially reveal the existence of non-universal structure at the GUT scale and thus provide important hints for the study of SUSY GUT models.

Then we showed that the current $B \to \phi K$ data, if it continues to hold in the future, will signal the first significant breakdown of the Standard Model and mSUGRA. The important consequence is that, in order to satisfy experimental data, one needs to construct a more complicated SUGRA model, e.g. with non-universal terms at the GUT scale, which may have very different signals in accelerator experiments. In particular, the only natural way to account for both $\sin 2\beta_{\phi K_S}$ and the branching ratios for $B \to \phi K$ was to add off diagonal elements mixing the second and third generations in the A soft breaking mass. This will provide important guidance to our future research on SUSY GUT models and for string models.

We then considered a model based on Horava-Witten M-Theory. We showed that this model can give a reasonable explanation to the origin of the SM mass spectrum. The hierarchy of quark and lepton masses arise in the model from 5-

branes being placed a distance d_n from the distant orbifold plane. The choice of $d_n \approx 0.1$ then replaces the phenomenological Wolfenstein parameter, producing the mass hierarchy naturally. We further investigated the possibility to accommodate the current neutrino data in this model. A new mechanism was proposed for this purpose by assuming the existance of right handed neutrinos which could give rise to cubic holomorphic contributions to the Kahler potential. When supersymmetry breaks, neutrino masses of the right size occur and the current neutrino data can be well satisfied in this model.

In short, SUSY is phenomenology that can bridge experiments and fundamental theory. It is useful in planing experiments and examining experimental data. Results obtained can then be used for further theoretical investigation.

REFERENCES

[1] K. Hagiwara, K. Hikasa, K. Nakamura, M. Tanabashi, M. Aguilar-Benitez, et al., Phys. Rev. D66 (2002) 010001.

[2] K.R. Dienes and C. Kolda, Perspectives on Supersymmetry, edited by G.L. Kane, World Scientific, 1998.

[3] G. Eigen, R. Gaitskell, G. D. Kribs and K. T. Matchev, eConf C010630 (2001) P342, hep-ph/0112312.

[4] Super-Kamiokande Collaboration, Y. Fukuda et al., Phys. Rev. Lett. 81 (1998) 1562, hep-ex/9807003.

[5] SNO Collaboration, Q.R. Ahmad et al., Phys. Rev. Lett. 87 (2001) 071301, nucl-ex/0106015.

[6] Muon g-2 Collaboration, G.W. Bennett et al., Phys. Rev. Lett. 89 (2002) 101804, hep-ex/0208001.

[7] Muon g-2 Collaboration, G.W. Bennett et al., Phys. Rev. Lett. 92 (2004), 161802, hep-ex/0401008.

[8] BABAR Collaboration, B. Aubert et al., Phys. Rev. Lett. 89 (2002) 201802, hep-ex/0207042.

[9] Belle Collaboration, K. Abe et al., Phys. Rev. Lett. 91 (2003) 261602, hep-ex/0308035.

[10] R. Arnowitt, A. Chamseddine and P. Nath, Applied N=1 Supergravity, World Scientific, Singapore, 1984.

[11] H. Haber and G. Kane, Phys. Rep. 117 (1985) 75.

[12] H.P. Nilles, Phys. Rep. 110 (1984) 1.

[13] D. J. H. Chung, L. L. Everett, G. L. Kane, S. F. King, J. Lykken and L. T. Wang, (2003), hep-ph/0312378.

[14] M. Quiros, (2003), hep-ph/0302189.

[15] D. Bailin and A. Love, Supersymmetric Gauge Field Theory and String Theory, Institute of Physics Publishing, Bristol, UK, 1994.

[16] S.P. Martin, (1997), hep-ph/9709356.

[17] H.E. Haber, Nucl. Phys. Proc. Suppl. 62 (1998) 469, hep-ph/9709450.

[18] J. Bagger and J. Wess, Supersymmetry and Supergravity, World Scientific, Singapore, 1990.

[19] A.H. Chamseddine, R. Arnowitt and P. Nath, Phys. Rev. Lett. 49 (1982) 970.

[20] R. Barbieri, S. Ferrara and C.A. Savoy, Phys. Lett. B119 (1982) 343.

[21] L.J. Hall, J. Lykken and S. Weinberg, Phys. Rev. D27 (1983) 2359.

[22] P. Nath, R. Arnowitt and A.H. Chamseddine, Nucl. Phys. B227 (1983) 121.

[23] L.E. Ibanez and C. Lopez, Nucl. Phys. B233 (1984) 511.

[24] L.E. Ibanez, C. Lopez and C. Munoz, Nucl. Phys. B256 (1985) 218.

[25] V.D. Barger, M.S. Berger and P. Ohmann, Phys. Rev. D49 (1994) 4908, hep-ph/9311269.

[26] S.P. Martin and M.T. Vaughn, Phys. Rev. D50 (1994) 2282, hep-ph/9311340.

[27] H.E. Haber, R. Hempfling and A.H. Hoang, Z. Phys. C75 (1997) 539, hep-ph/9609331.

[28] R. Rattazzi and U. Sarid, Phys. Rev. D53 (1996) 1553, hep-ph/9505428.

[29] M. Carena, M. Olechowski, S. Pokorski and C. E. M. Wagner, Nucl. Phys. B426 (1994) 269, hep-ph/9402253.

[30] F. Gabbiani and A. Masiero, Nucl. Phys. B322 (1989) 235.

[31] M. Carena and H.E. Haber, Prog. Part. Nucl. Phys. 50 (2003) 63, hep-ph/0208209.

[32] ALEPH Collaboration, R. Barate et al., Phys. Lett. B565 (2003) 61, hep-ex/0306033.

[33] M. Nakao, (2003), hep-ex/0312041.

[34] P. Gambino and M. Misiak, Nucl. Phys. B611 (2001) 338, hep-ph/0104034.

[35] CLEO Collaboration, T.E. Coan et al., Phys. Rev. Lett. 86 (2001) 5661, hep-ex/0010075.

[36] G. Jungman, M. Kamionkowski and K. Griest, Phys. Rept. 267 (1996) 195, hep-ph/9506380.

[37] H. V. Peiris, E. Komatsu, L. Verde, D.N. Spergel, C.L. Bennett, et al., Astrophys. J. Suppl. 148 (2003) 213, astro-ph/0302225.

[38] E. de Rafael, (2002), hep-ph/0208251.

[39] R. Arnowitt and B. Dutta, (2002), hep-ph/0210339.

[40] M. Davier, S. Eidelman, A. Hocker and Z. Zhang, Eur. Phys. J. C31 (2003) 503, hep-ph/0308213.

[41] E. Accomando, R. Arnowitt and B. Dutta, Phys. Rev. D61 (2000) 115003, hep-ph/9907446.

[42] E. Accomando, R. Arnowitt and B. Dutta, Phys. Rev. D61 (2000) 075010, hep-ph/9909333.

[43] R. Arnowitt, B. Dutta and B. Hu, (2003), hep-ph/0310103.

[44] L.H. Ryder, Quantum Field Theory, Cambridge University Press, 1985.

[45] J. Schwinger, Phys. Rev. 73 (1948) 416.

[46] A. Nyffeler, (2003), hep-ph/0305135.

[47] P. Fayet, Unification of the Fundamental Particle Interactions, S. Ferrara, J. Ellis and P. van Nieuwenhuizen (Eds.), Plenum, New York, 1980.

[48] J.A. Grifols and A. Mendez, Phys. Rev. D26 (1982) 1809.

[49] J.R. Ellis, J.S. Hagelin and D.V. Nanopoulos, Phys. Lett. B116 (1982) 283.

[50] R. Barbieri and L. Maiani, Phys. Lett. B117 (1982) 203.

[51] S. Ferrara and E. Remiddi, Phys. Lett. B53 (1974) 347.

[52] T. C. Yuan, R. Arnowitt, A. H. Chamseddine and P. Nath, Zeit. Phys. C26 (1984) 407.

[53] J.R. Ellis, S. Kelley and D.V. Nanopoulos, Phys. Lett. B249 (1990) 441.

[54] R. Arnowitt, B. Dutta, B. Hu and Y. Santoso, Phys. Lett. B505 (2001) 177, hep-ph/0102344.

[55] D.A. Kosower, L.M. Krauss and N. Sakai, Phys. Lett. B133 (1983) 305.

[56] J.L. Lopez, D.V. Nanopoulos and X. Wang, Phys. Rev. D49 (1994) 366, hep-ph/9308336.

[57] G. Degrassi, P. Gambino and G.F. Giudice, JHEP 12 (2000) 009, hep-ph/0009337.

[58] M. Carena, D. Garcia, U. Nierste and C. E. M. Wagner, Phys. Lett. B499 (2001) 141, hep-ph/0010003.

[59] R. Arnowitt, B. Dutta and Y. Santoso, Nucl. Phys. B606 (2001) 59, hep-ph/0102181.

[60] M. Drees, Y. G. Kim, T. Kobayashi and M. M. Nojiri, Phys. Rev. D63 (2001) 115009, hep-ph/0011359.

[61] J.R. Ellis, A. Ferstl and K.A. Olive, Phys. Rev. D63 (2001) 065016, hep-ph/0007113.

[62] M.E. Gomez and J.D. Vergados, Phys. Lett. B512 (2001) 252, hep-ph/0012020.

[63] J. R. Ellis, T. Falk, G. Ganis, K. A. Olive and M. Srednicki, Phys. Lett. B510 (2001) 236, hep-ph/0102098.

[64] A. Czarnecki and W.J. Marciano, Phys. Rev. D64 (2001) 013014, hep-ph/0102122.

[65] N.E. Mavromatos, (2004), hep-ph/0402005.

[66] A. Ali, (2003), hep-ph/0312303.

[67] R. Arnowitt, B. Dutta and B. Hu, Phys. Rev. D68 (2003) 075008, hep-ph/0307152.

[68] A.J. Buras, (2002), hep-ph/0210291.

[69] Y. Grossman and M.P. Worah, Phys. Lett. B395 (1997) 241, hep-ph/9612269.

[70] BABAR Collaboration, B. Aubert et al., (2002), hep-ex/0207070.

[71] Belle Collaboration, K. Abe et al., (2002), hep-ex/0207098.

[72] BELLE Collaboration, K. Abe et al., Phys. Rev. D67 (2003) 031102, hep-ex/0212062.

[73] BABAR Collaboration, G. Hamel De Monchenault, (2003), hep-ex/0305055.

[74] BABAR Collaboration, B. Aubert et al., (2004), hep-ex/0403026.

[75] T.E. Browder, (2003), hep-ex/0312024.

[76] Heavy Flavor Averaging Group (HFAG), http://www.slac.stanford.edu/xorg/hfag/.

[77] CLEO Collaboration, R.A. Briere et al., Phys. Rev. Lett. 86 (2001) 3718, hep-ex/0101032.

[78] M. Beneke, G. Buchalla, M. Neubert and C. T. Sachrajda, Phys. Rev. Lett. 83 (1999) 1914, hep-ph/9905312.

[79] M. Beneke, G. Buchalla, M. Neubert and C. T. Sachrajda, Nucl. Phys. B591 (2000) 313, hep-ph/0006124.

[80] M. Beneke, G. Buchalla, M. Neubert and C. T. Sachrajda, Nucl. Phys. B606 (2001) 245, hep-ph/0104110.

[81] D. s. Du, H. j. Gong, J. f. Sun, D. s. Yang and G. h. Zhu, Phys. Rev. D65 (2002) 094025, hep-ph/0201253.

[82] D. s. Du, J. f. Sun, D. s. Yang and G. h. Zhu, Phys. Rev. D67 (2003) 014023, hep-ph/0209233.

[83] G.h. Zhu (Beijing, Inst. High Energy Phys. and KEK, Tsukuba), private communication.

[84] A. Ali, G. Kramer and C.D. Lu, Phys. Rev. D58 (1998) 094009, hep-ph/9804363.

[85] A.J. Buras, (1998), hep-ph/9806471.

[86] A. Ali, G. Kramer and C.D. Lu, Phys. Rev. D59 (1999) 014005, hep-ph/9805403.

[87] A. Khodjamirian, R. Ruckl, S. Weinzierl, C. W. Winhart and O. I. Yakovlev, Phys. Rev. D62 (2000) 114002, hep-ph/0001297.

[88] P. Ball, JHEP 09 (1998) 005, hep-ph/9802394.

[89] A. Ali, V.M. Braun and H. Simma, Z. Phys. C63 (1994) 437, hep-ph/9401277.

[90] L. Wolfenstein, Phys. Rev. Lett. 51 (1983) 1945.

[91] M. Ciuchini, G. D'Agostini, E. Franco, V. Lubicz, G. Martinelli, et al., JHEP 07 (2001) 013, hep-ph/0012308.

[92] M. Ciuchini, Nucl. Phys. Proc. Suppl. 109B (2002) 307, hep-ph/0112133.

[93] T. Falk and K.A. Olive, Phys. Lett. B375 (1996) 196, hep-ph/9602299.

[94] T. Ibrahim and P. Nath, Phys. Lett. B418 (1998) 98, hep-ph/9707409.

[95] T. Ibrahim and P. Nath, Phys. Rev. D57 (1998) 478, hep-ph/9708456.

[96] G. L. Kane, P. Ko, H. b. Wang, C. Kolda, J. h. Park and L. T. Wang, Phys. Rev. Lett. 90 (2003) 141803, hep-ph/0304239.

[97] M. Ciuchini, L. Conti, A. Donini, E. Franco, V. Gimenez, et al., JHEP 10 (1998) 008, hep-ph/9808328.

[98] R. Arnowitt and B. Dutta, Nucl. Phys. B592 (2001) 143, hep-th/0006172.

[99] R. Arnowitt, B. Dutta and B. Hu, Nucl. Phys. B682 (2004) 347, hep-th/0309033.

[100] H. Georgi and C. Jarlskog, Phys. Lett. B86 (1979) 297.

[101] P. Ramond, R.G. Roberts and G.G. Ross, Nucl. Phys. B406 (1993) 19, hep-ph/9303320.

[102] P. Horava and E. Witten, Nucl. Phys. B460 (1996) 506, hep-th/9510209.

[103] P. Horava and E. Witten, Nucl. Phys. B475 (1996) 94, hep-th/9603142.

[104] M. Gell-Mann, P. Ramond and R. Slansky, Supergravity, P. van Nieuwenhuizen and D. Freedman (Eds.), North Holland Publ. Co., North Holland, Amsterdam, 1979.

[105] T. Yanagida, Prog. Theor. Phys. 64 (1980) 1103.

[106] R.N. Mohapatra and G. Senjanovic, Phys. Rev. Lett. 44 (1980) 912.

[107] Z. Maki, M. Nakagawa and S. Sakata, Prog. Theor. Phys. 28 (1962) 870.

[108] M.C. Gonzalez-Garcia and C. Pena-Garay, Phys. Rev. D68 (2003) 093003, hep-ph/0306001.

[109] A. Lukas, B.A. Ovrut and D. Waldram, JHEP 04 (1999) 009, hep-th/9901017.

[110] E. Witten, Nucl. Phys. B471 (1996) 135, hep-th/9602070.

[111] K. Schubert, talk given at XXI International Symposium on Lepton and Photon Interactions at High Energies, Fermilab, Batavia, Illinois (2003), http://conferences.fnal.gov/lp2003/program/S6/schubert_s06.pdf.

[112] Super-Kamiokande Collaboration, S. Fukuda et al., Phys. Rev. Lett. 85 (2000) 3999, hep-ex/0009001.

[113] Super-Kamiokande Collaboration, M.B. Smy et al., Phys. Rev. D69 (2004) 011104, hep-ex/0309011.

[114] SNO Collaboration, Q.R. Ahmad et al., Phys. Rev. Lett. 89 (2002) 011301, nucl-ex/0204008.

[115] SNO Collaboration, Q.R. Ahmad et al., Phys. Rev. Lett. 89 (2002) 011302, nucl-ex/0204009.

[116] KamLAND Collaboration, K. Eguchi et al., Phys. Rev. Lett. 90 (2003) 021802, hep-ex/0212021.

[117] M.C. Gonzalez-Garcia and Y. Nir, Rev. Mod. Phys. 75 (2003) 345, hep-ph/0202058.

[118] D.N. Spergel, L. Verde, Hiranya V. Peiris, E. Komatsu, et al., Astrophys. J. Suppl. 148 (2003) 175, astro-ph/0302209.

[119] G. L. Fogli, E. Lisi, A. Marrone and D. Montanino, Phys. Rev. D67 (2003) 093006, hep-ph/0303064.

[120] S.M. Bilenky and C. Giunti, Phys. Lett. B444 (1998) 379.

[121] G.F. Giudice and A. Masiero, Phys. Lett. B206 (1988) 480.

[122] E. Lima, B. A. Ovrut, J. Park and R. Reinbacher, Nucl. Phys. B614 (2001) 117, hep-th/0101049.

[123] G.W. Moore, G. Peradze and N. Saulina, Nucl. Phys. B607 (2001) 117, hep-th/0012104.

[124] G. Curio and A. Krause, Nucl. Phys. B643 (2002) 131, hep-th/0108220.

[125] E.I. Buchbinder and B.A. Ovrut, (2003), hep-th/0310112.

[126] H.Y. Cheng, Phys. Rept. 158 (1988) 1.

[127] P.J. Franzini, Phys. Rept. 173 (1989) 1.

[128] H.K. Quang and X.Y. Pham, Elementary Particles and Their Interactions: Concepts and Phenomena, Springer-Verlag, Berlin, Germany, 1998.

[129] M. Bander, D. Silverman and A. Soni, Phys. Rev. Lett. 43 (1979) 242.

[130] A.J. Buras and L. Silvestrini, Nucl. Phys. B548 (1999) 293, hep-ph/9806278.

[131] H.n. Li, Czech. J. Phys. 53 (2003) 657, hep-ph/0303116.

[132] D.s. Du, D.s. Yang and G.h. Zhu, Phys. Rev. D64 (2001) 014036, hep-ph/0103211.

[133] M. Beneke and M. Neubert, Nucl. Phys. B675 (2003) 333, hep-ph/0308039.

APPENDIX A

PARAMETERS OF THE STANDARD MODEL

The SM is built on the $SU(3)_C \times SU(2)_L \times U(1)_Y$ symmetry group (where subscript "C", "L" and "Y" are short for "color", "left" and "hypercharge"). Its particle spectrum can be divided into three sectors, i.e.

1. Gauge sector composed of gauge bosons, i.e. G^a, W^i and B, corresponding to $SU(3)_C$, $SU(2)_L$ and $U(1)_Y$ separately,

2. Fermion sector containing three generations of quarks ($q_L = (u_L\ , d_L)$, u_R and d_R) and leptons ($l_L = (\nu_L\ \ e_L)$, e_R) (Generation index and color index are suppressed here. Subscripts "L" and "R" correspond to left-handed and right-handed.).

3. Higgs sector containing the Higgs doublet $H = (H^0\ , H^-)$.

All the particles gain masses through spontaneously breaking of

$$SU(3)_C \times SU(2)_L \times U(1)_Y \Rightarrow SU(3)_C \times U(1)_{EM} \tag{A.1}$$

when the Higgs field develops a non-zero vacuum expectation value (VEV)

$$\langle H \rangle = \begin{pmatrix} v \\ 0 \end{pmatrix} \ . \tag{A.2}$$

In particular, after the spontaneously symmetry breaking (SSB), the Yukawa terms

$$\mathcal{L}_{\rm Y} = Y^{(u)} \bar{q}_L H^+ u_R + Y^{(d)} \bar{q}_L H d_R + Y^{(e)} \bar{l}_L H e_R \tag{A.3}$$

give rise to fermion masses except for the neutrinos. (See Chapter V for a discussion on neutrino masses) The fermionic contribution to the Lagrangian is

$$\begin{aligned} \mathcal{L}_{\rm fm} &= -Y^{(u)} v \bar{u}_L u_R + Y^{(d)} v \bar{d}_L d_R + Y^{(e)} v \bar{e}_L e_R \\ &= M^{(u)} \bar{u}_L u_R + M^{(d)} \bar{d}_L d_R + M^{(e)} \bar{e}_L e_R \end{aligned} \tag{A.4}$$

where $M^{(u,d,e)}$ are mass matrices in the flavor basis and thus need to be diagonalized in order to obtain physical states. After the diagonalization of M^u and M^d, the quark mixing Cabibbo-Kobayashi-Maskawa (CKM) matrix will appear in the charged-current interactions. (There is no lepton mixing in the lepton sector since neutrinos are strictly massless in the SM, as shown in (A.4).) In the flavor basis, the charged currents are diagonal

$$\mathcal{L}_{\rm CC} = -\frac{g}{\sqrt{2}}(J^+_\mu W^\mu + \text{h.c.}) \tag{A.5}$$

where $W = (W^1 - iW^2)/\sqrt{2}$ being the physical W boson and

$$J^+_\mu = \bar{u}_L \gamma_\mu d_L \ . \tag{A.6}$$

The diagonalization of M^u and M^d changes the flavor basis to the mass (physical) basis and then

$$J^+_\mu = \bar{u}_L \gamma_\mu V_{\rm CKM} d_L \tag{A.7}$$

where $V_{\rm CKM} = U^+_L D_L$ with unitary matrices U_L and D_L diagonalizing M^u and M^d (of course, u_R and d_R need to be rotated at the same time). In the case of three generations, $V_{\rm CKM}$ is a 3×3 unitary matrix and can be parameterized by four physical quantities including three real rotation angles θ_{ij} $(i,j = 1,2,3)$ plus one complex phase δ [1]

$$\begin{aligned} V_{CKM} &= \begin{pmatrix} V_{ud} & V_{us} & V_{ub} \\ V_{cd} & V_{cs} & V_{cb} \\ V_{td} & V_{ts} & V_{tb} \end{pmatrix} \\ &= \begin{pmatrix} c_{12}c_{13} & s_{12}c_{13} & s_{13}e^{-i\delta} \\ -s_{12}c_{23} - c_{12}s_{23}s_{13}e^{i\delta} & c_{12}c_{23} - s_{12}s_{23}s_{13}e^{i\delta} & s_{23}c_{13} \\ s_{12}s_{23} - c_{12}c_{23}s_{13}e^{i\delta} & -c_{12}s_{23} - s_{12}c_{23}s_{13}e^{i\delta} & c_{23}c_{13} \end{pmatrix} \end{aligned} \tag{A.8}$$

Here $s_{ij} = \sin\theta_{ij}$ and $c_{ij} = \cos\theta_{ij}$. Phase δ is the only source of CP violations in the SM. In the framework of the SM, the CKM matrix elements cannot be determined theoretically and thus have to be determined from experiments (see Chapter IV for a brief discussion on current experimental status).

We can now count the number of physical parameters in the SM

- 6 quark masses and 3 lepton masses
- 3 gauge couplings
- 4 CKM parameters
- 2 Higgs potential parameters

which add up to 18 parameters in total or 19 if we add θ_{QCD} [126], as mentioned in chapter I.

APPENDIX B

CP ASYMMETRIES OF $B \to \phi K$ DECAYS

In general, there are three types of CP violations in B decays:

1. (Direct) CP violation in decay, which occurs when the amplitudes of a decay and its CP-conjugate are not equal, e.g. $\mathcal{A}(B^+ \to \phi K^+) \neq \mathcal{A}(B^- \to \phi K^-)$,

2. (Indirect) CP violation in $B^0 - \bar{B}^0$ mixing when the mass eigenstates are different from CP eigenstates,

3. CP violation in the interference between decays and mixing.

We shall concentrate on the $B^0 \to \phi K_S$ decay discussed in Chapter IV. Since it belongs to the third type, we start with $B^0 - \bar{B}^0$ mixing.

For $B^0\bar{B}^0$ system, the two mass eigenstates, B_L and B_H with masses M_L and M_H respectively, can be written as linear combinations of B^0 and $\bar{B}^0$ [127]

$$\begin{aligned} |B_L\rangle &= p|B^0\rangle + q|\bar{B}^0\rangle \\ |B_H\rangle &= p|B^0\rangle - q|\bar{B}^0\rangle \end{aligned} \tag{B.1}$$

with $|p^2| + |q^2| = 1$. p and q are determined by interactions mixing B^0 and $\bar{B}^0$, e.g. electroweak interactions and possible new physics interactions. Ignoring the difference between the decay widths of B_L and B_H, the time evolution of the mass eigenstates is given by

$$\begin{aligned} |B_L^0(t)\rangle &= e^{-(\Gamma/2+iM_L)t}|B_L^0(0)\rangle \ , \\ |B_H^0(t)\rangle &= e^{-(\Gamma/2+iM_H)t}|B_H^0(0)\rangle \ . \end{aligned} \tag{B.2}$$

Now consider a system with pure $|B^0\rangle$ or $|\bar{B}^0\rangle$ at $t = 0$. At a later time t, the system can then be described by

$$\begin{aligned} |B^0_{\rm phys}(t)\rangle &= f_+(t)|B^0\rangle + \frac{q}{p} f_-(t)|\bar{B}^0\rangle \ , \\ |\bar{B}^0_{\rm phys}(t)\rangle &= \frac{p}{q} f_-(t)|B^0\rangle + f_+(t)|\bar{B}^0\rangle \end{aligned} \tag{B.3}$$

where

$$\begin{aligned} f_+(t) &= e^{-(\Gamma/2+iM_B)t}\cos(\Delta M_B t/2) \ , \\ f_-(t) &= e^{-(\Gamma/2+iM_B)t} i \sin(\Delta M_B t/2) \end{aligned} \tag{B.4}$$

and

$$M_B \equiv (M_H + M_L)/2 \ ; \ \ \Delta M_B \equiv M_H - M_L \ . \tag{B.5}$$

Substituting back to the definition of the time dependent CP asymmetry in (4.2) and noticing that ϕK_S is CP odd and q/p can be set to $\exp(-2i\beta)$ because $|q/p| \cong 1$ for the B system [128], one recoveries the result given there.

In addition, in decay amplitudes (e.g. (4.4)), there are two types of phases that may appear, i.e. weak phases and strong phases. Weak phases are phases from the Lagrangian, e.g. the CKM phase in the SM and phases from the soft SUSY breaking parameters in SUSY models. On the contrary, strong phases do not violate CP and thus do not change sign in CP conjugate amplitudes. The origin of strong phases is model dependent, e.g. via the Bander-Silverman-Soni (BSS) mechanism [129] in which strong phases can arise in one loop diagrams. Strong phases are very important for direct CP violations since, as shown in (4.10) and (4.11), $\mathcal{A}_{CP}$ can be non-zero only when $\bar{A}/A \neq 0$, which can happen only when two different strong phase and weak phases are present.

APPENDIX C

QCD FACTORIZATION

As mentioned in Chapter IV, for exclusive non-leptonic B decays, the calculation of decay amplitudes requires the evaluation of the matrix elements between hadronic states, e.g. $\langle M_1 M_2|O_i|B\rangle$ for B decays. Previously the method most used was naive factorization (NF) in which the matrix element is approximated by a product of two matrix elements of current operators, i.e.

$$\langle M_1 M_2|O_i|B\rangle \simeq \langle M_1|J_1|0\rangle\langle M_2|J_2|B\rangle \ , \tag{C.1}$$

and then parametrized into meson decay constants and transition form factors. Despite the fact that NF can provide good approximations for many decay modes, it has some intrinsic problems. Theoretically the most serious one is its scale dependence, which can be seen by noticing that the matrix elements in NF are scale independent but, on the other hand, the Wilson coefficients C_i's are scale dependent and hence lead to scale dependent amplitudes, i.e. $\mathcal{A} \propto C_i(\mu)\langle M_1 M_2|O_i|B\rangle$. Another problem is that is that no strong phase can be produced in NF, as implied by (C.1), and hence direct CP is totally missing in NF.

To overcome the problems of NF, some solutions have been proposed. One of them is called generalized factorization [84] in which the scale dependence of C_i's are compensated by additional scale dependent factors from the radiative corrections to O_i's. The matrix elements are still calculated by the NF method, i.e. approximating $\langle M_1 M_2|O_i|B\rangle$ by a product of a decay constant and a form factor. This factorization approach, although used in many analyses, still has some unresolved problems, e.g. gauge dependence (for more details, see, e.g. [130]). Another two approaches

where the problems in NF are resolved are perturbative QCD (PQCD) and QCD factorization (QCDF). A thorough review with a detailed comparison between those approaches can be found in [131]. Here we concentrate on QCD factorization (or the BBNS approach [78, 79, 80]).

In QCDF, factorization means the separation of long-distance (soft) contributions from short-distance (hard) contributions, as demonstrated in the following QCDF factorization formula for the decay of B meson into two light mesons [79]

$$\begin{aligned}\langle M_1 M_2|\mathcal{O}_i|\bar{B}\rangle &= F^{B\to M_1}\int_0^1 du\, T_i^I(u)\,\Phi_{M_2}(u) \;+\; (M_1 \leftrightarrow M_2) \\ &\quad + \int_0^1 d\xi du dv\, T_i^{II}(\xi,u,v)\,\Phi_B(\xi)\,\Phi_{M_1}(v)\,\Phi_{M_2}(u) \qquad \text{(C.2)}\end{aligned}$$

where $F^{B\to M_{1,2}}$ is a $B\to M_{1,2}$ form factor, Φ's are light-cone distribution amplitudes (LCDAs) and T^I and T^{II} are hard-scattering kernels. In QCDF, both transition form factors and LCDAs are considered to be dominated by soft contributions and hence have to be calculated by non-perturbative methods or determined experimentally. (On the contrary, in PQCD form factors have been claimed to be perturbatively calculable [131].) Hard-scattering kernels are the short-distance part and can be calculated perturbatively. The consistency of the QCDF method has been argued and explicitly shown by examples in [79] and [132].

Fig. 10 gives a graphic representation of (C.2) and can be understood as follows. The light mesons produced in 2-body B decays are energetic and move apart very fast. This decoupling makes it possible to calculate perturbatively the decay vertex which are represented by $T^{I,II}$ in (C.2). Decoupled mesons are then described by their LCDAs as meson states are intrinsically non-perturbative. The first term in (C.2) describes the situation in which the soft spectator quark is not involved in the decay vertex and hence the $B\to M_1$ transition is considered as a soft process and

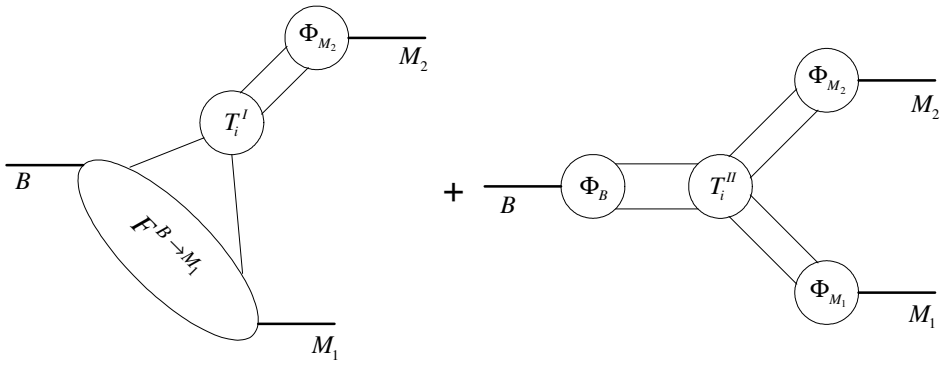

Fig. 10. Graphical representation of the factorization formula (C.2)

described by a form factor [79]. The second term describes the case with interactions occuring between the outgoing energetic meson and the spectator quark.

Explicit vertex diagrams and calculations can be found in [79] and [132] and a comprehensive formula list for $B \to PP$, PV is given in [133]. As shown in (4.15), for convenience, in most QCDF papers, decay amplitudes are usually presented in terms of factorized matrix elements (i.e., the right hand side of (C.1)). However, QCDF should not be taken as a simple extension to NF. At least, the second term in the right hand side of (C.2) (which is a term at the next-to-leading order or the first order of $\alpha_s \equiv g_s^2/4\pi$) is not present in NF. Nevertheless, QCDF does agree with NF in the leading order (or the zeroth order of α_s) [79], which can be considered as one consistency check if NF is viewed as the correct first order approximation.

Although QCDF is an important advance, it is far from the end of the story. For example, there are still infrared divergences when high order contributions to the LCDAs are taken into account, causing the dependence on some phenomenological parameters (i.e. ρ and ϕ in (4.17), see also Fig. 7 in Chapter 4 and discussion there). This considerably limits its predictive power. In addition, QCDF does not have an entirely self-consistent treatment for the annihilation contributions. Therefore, it needs further investigation and is to be used with justification, especially to avoid the

overusing or abusing those unexplained parameters mentioned above.

VITA

Bo Hu received his B.S. degree in 1992 from Southwestern Jiaotong University, China. In 1998, he earned his M.S. degree from Beijing Normal University, China. He came to Texas A&M University in the same year to continue his studies in physics and earned a Ph.D. in August 2004. He can be contacted through No. 711 Factory, Residents' committee No. 8-604, Shashi, Jingzhou, Hubei, 434007, China.

The typist for this thesis was Bo Hu.